Transportation Research Part C 143 (2022) 103793

Contents lists available at ScienceDirect

Transportation Research Part C

journal homepage: www.elsevier.com/locate/trc

Optimization of service frequency and vehicle size for automated bus systems with crowding externalities and travel time stochasticity

Mohammad Sadrani [a], Alejandro Tirachini [b,c], Constantinos Antoniou [a,*]

[a] Chair of Transportation Systems Engineering, TUM School of Engineering and Design, Technical University of Munich, Munich 80333, Germany
[b] Transport Engineering Division, Civil Engineering Department, Universidad de Chile, Chile
[c] Instituto Sistemas Complejos de Ingeniería, Chile

ARTICLE INFO

Keywords:
Vehicle automation
Public transport
Total cost minimization
In-vehicle crowding
Travel time stochasticity

ABSTRACT

Public transport is considered as one of the most suitable candidates to benefit from autonomous driving technologies. In this research, we develop a mathematical modeling framework to optimize service frequency and vehicle size for automated bus systems, while accounting for both user and operator costs. We explicitly consider travel time stochasticity, time-dependent passenger flows, vehicle capacity limitations (extra waiting time due to denied boarding), and in-vehicle discomfort externalities for both sitting and standing passengers at a microscopic level. We attempt to provide a thorough assessment of the service and cost implications of the deployment of automated buses. Hence, a broad range of experiments are simulated by combining different deployment cases: (i) vehicle technology (human-driven or automated vehicles), (ii) travel time assumptions (deterministic or stochastic travel times), and (iii) crowding externalities (considering or ignoring in-vehicle crowding costs). The model applicability is assessed on two real-world bus corridors in Regensburg (Germany) and Santiago (Chile). Results show that, with crowding externalities, optimal vehicle size is increased at a similar rate for both human-driven and automated bus services, whereas optimal service frequency is increased at a higher rate for automated buses. Thus, under optimal levels of supply, automated vehicles are operated with lower occupancy levels than human-driven vehicles, increasing the quality of service. Besides, the deployment of automated bus systems can significantly alleviate or eliminate denied boardings. The effects of automation on travel time volatility and dwell time regularity are studied. The consideration of stochastic travel times increases optimal frequencies at a higher rate for automated services relative to human-driven vehicles. Interestingly, we find that even though the operator benefits from automation are more pronounced in high-income countries (due to a greater potential for human driving cost savings), the final outcome is counterbalanced by the actual public transport demand level, because large user cost savings from automation are reachable in crowded routes even in situations in which labor costs are lower (as in developing countries).

* Corresponding author.
E-mail addresses: m.sadrani@tum.de (M. Sadrani), Alejandro.tirachini@ing.uchile.cl (A. Tirachini), c.antoniou@tum.de (C. Antoniou).

https://doi.org/10.1016/j.trc.2022.103793
Received 1 February 2022; Received in revised form 23 June 2022; Accepted 4 July 2022
Available online 31 July 2022

1. Introduction

The advent of automated vehicles with no need for human driving is expected to bring forth a wide range of effects to the transportation systems (Nair and Bhat, 2021). Public transport is considered as one of the most suitable candidates to benefit from automated driving capabilities. In urban bus operations, human driving costs (drivers' salaries) can account for the vast majority of the total operating costs of a bus system, e.g., between 30% and 70% of total bus operator costs in countries such as Japan, Australia, Chile and Germany (Abe, 2019; Tirachini and Antoniou, 2020). Nonetheless, human-related driving costs can be significantly saved with automated bus operations equipped with autonomous driving technologies, due to the elimination of (at least a part of) drivers' wages. Based on the levels of driving automation defined by the Society of Automotive Engineers (SAE), future vehicles can operate with no need for human driving under certain conditions at Level 4, and under all conditions at Level 5 (SAE, 2018). Hence, it is expected that the public transport industry and service will be widely affected by automation capabilities in the next years, at least for operation in segregated environments such as busways.

The deployment of automated public transport systems for improving the level of service and reducing the social costs of a public transportation service has emerged as a research topic in the past decade. Generally, people appear to be positive about the deployment of (future) automated bus systems (e.g., Alessandrini et al., 2011; Eden et al., 2017; Distler et al., 2018; Ceder, 2021). Thus far, a broad spectrum of connected and autonomous driving technologies have been evolved and introduced to automated public transport systems for providing more robust autonomous mobility services, such as bus platooning, lane-keeping, collision avoidance, bus precision docking (i.e., providing a stable distance between vehicles and platforms at stations), automated emergency braking, cooperative adaptive cruise control (CACC), vehicle-to-vehicle (V2V) and vehicle-to-infrastructure (V2I) communications (Lazarus et al., 2018; Lutin, 2018). Hence, beyond human driving cost savings with automation, it is expected that the deployment of automated vehicles can positively affect public transport systems in various aspects via leveraging full automation capabilities (Tirachini and Antoniou, 2020). As the technology matures, it is also predicted that the prices of connected and autonomous vehicle technologies will progressively reduce at certain annual rates within lower and upper bounds of 5% and 10% (Mosquet et al., 2015; Bansal and Kockelman, 2017), thereby providing a greater opportunity for urban public transportation agencies to accelerate the deployment of fully automated transport systems on their routes with lower capital costs in the next decades.

In recent years, a growing number of studies have focused on the optimal design and deployment of automated bus services to minimize the social costs of public transport services. Zhang et al. (2019) proposed a total cost minimization model to find the optimal bus frequency and size for fleets of conventional, semi-automated, and fully-automated buses on a generic hub-and-branch network. Given the reduction or elimination of in-vehicle crew costs with automation, results showed that automated vehicle solutions optimally suggest a higher service frequency and a smaller vehicle size. This result has been also replicated by Fielbaum (2019), and Tirachini and Antoniou (2020). Overall, despite the increase of capital costs due to the inclusion of automation technologies inside buses, fully-automated buses exhibit great potential through the reduction of operating and waiting costs. Fielbaum (2019) proposed a feeder–trunk automated vehicle public transport model, taking advantage of vehicle automation and mixing on-demand systems for local trips (feeder) with a more traditional system for longer trips (trunk). It was found that the technology of automation pushes the system toward providing larger fleets of smaller vehicles. Tirachini and Antoniou (2020) presented an optimization model to assess the impacts of vehicle automation on optimal vehicle size, service frequency, fare, subsidy, and degree of economies of scale. The model was tested using data from Chile and Germany, taken as illustrative examples of developing and developed countries. Results showed that automated services benefit users, through a reduction of waiting times and optimal fares, operators, through a reduction of operating cost, and the public sector, through a reduction of the first-best optimal subsidy per bus trip. Moreover, it was found that the benefits of automation are more prominent in countries where drivers' wages are higher (such as Germany relative to Chile), due to larger savings of human-related driving costs with automation.

Hatzenbühler et al. (2020) proposed an analytical model to optimize frequency and vehicle capacity for human-driven and automated bus fleets, while considering the sum of passenger and operator costs on a weighted normalized basis, where weighting factors allow for the analysis of passenger- and operator-oriented solutions. The model was applied to a real-life case study in Kista (Stockholm, Sweden), and the results showed that automated bus services have the potential to attract passengers through improved service provision. Badia and Jenelius (2021) assessed the possible effects of vehicle automation and electrification on the design and optimization of feeder transit services in suburban areas. For this purpose, an analytical model was proposed based on continuum approximations, while considering and comparing the applicability of two different operating strategies of feeder transit systems: parallel fixed lines and door-to-door trips. The authors modeled user costs and operator costs, while considering the economic effects of new vehicle technologies on system cost structures. The findings showed that the effect of automation on the applicability between the two feeder options is clearly more significant than the effect of electrification.

To determine the optimal frequencies of autonomous minibuses when serving several sublines, Gkiotsalitis et al. (2022) developed a stochastic optimization model as a mixed-integer linear programming (MILP) formulation, while accounting for the stochasticity of passenger demand. The problem objective was to minimize the sum of operational and passenger waiting time costs. The model performance was tested under deterministic and stochastic demand scenarios, showing 10–40% operational cost savings when assigning optimal frequency solutions to sublines. Besides, to improve the level of service and reduce running costs at operational planning levels, some scholars have attempted to create new mathematical formulations for the optimization of skip-stop tactics and other operational strategies (such as holding and speed changing), while accounting for automated driving capabilities in public transport services (Cao et al., 2019; Cao and Ceder, 2019).

As for the operation with mixed fleets, Dai et al. (2020) developed an integer nonlinear programming model to optimize vehicle types and dispatch times for a mixed fleet of human-driven and automated buses. The authors assumed that the capacity of automated

buses can be dynamically changed at terminals through assembling/dissembling minibus modules. The model objective was to minimize passenger and bus operating costs. Results showed that passenger costs can be reduced significantly using dynamic dispatching solutions. Tian et al. (2020) proposed a stochastic programming model to optimize the fleet size required for mixed fleet operations with conventional and automated vehicles in a bus network, while aiming to minimize passenger waiting times and operator costs under stochastic demand conditions. Results confirmed the benefits of automated buses that can be allocated to different bus lines in a more flexible manner.

The extant literature on public transport design and optimization with automated vehicles still has several relevant research questions open for inquiry. We can first mention the impacts of in-vehicle crowding externalities on determining the optimal frequency and vehicle size for an automated bus system. Two effects of passenger crowding deserve particular attention in the comparison of human-driven vs. automated vehicles: the crowding discomfort as increasing the value of travel time savings, and the possibility of passengers not being able to board vehicles due to capacity constraints. Second, despite the stochastic nature of public transport operations, the possible effects of automation on travel time variability and dwell time regularity have not yet been extensively studied in the literature of automated bus operations. To fill these research gaps, we formulate a novel mathematical model for solving the problem of setting service frequency and vehicle size for automated or conventional human-driven bus systems. Accordingly, we formulate a comprehensive objective function, encompassing both user and operator costs, to minimize the total costs of a public transport service. Operator cost includes three elements: capital, driving, and running costs. User cost includes two elements: waiting time cost (initial waiting time, and extra waiting time due to failing to board), and in-vehicle time cost that is sensitive to on-board crowding levels. Under time-dependent OD demand volumes, we model spatial–temporal variations of passenger demand at a microscopic level (the actual number of passengers alighting and boarding each vehicle at each stop), allowing for capturing the actual variations of occupancy levels inside vehicles and the relevant impacts on (i) the level of on-board discomfort for both seated and standing passengers, and (ii) the travel time of users being left behind due to overcrowding. Besides, several constraints are modeled for a detailed simulation of urban bus operations, including vehicle movement, passenger-carrying capacity, and passenger flow constraints.

The objective of the model is to find the optimal service frequency and bus size for minimizing the total costs of a public transport service. Given time-dependent demand flows and stochastic travel times, we explicitly model on-board discomfort: the disutility of in-vehicle travel time (i.e., increasing the value of in-vehicle time savings) for both sitting and standing travelers inside vehicles (for a recent review, see Hörcher and Tirachini, 2021). Unlike previous studies on the matter of crowding valuation and optimal public transport supply (e.g., Tirachini et al., 2014), we measure crowding discomfort at a microscopic level (bus by bus), depending on the number of seated and standing passengers inside each bus at each route segment. For real-life applications, the model is tested on two bus corridors in Regensburg (Germany), and Santiago (Chile). For each case study, eight deployment scenarios are simulated under different combinations of (i) vehicle technology (human-driven or automated vehicles), (ii) travel time assumptions (deterministic or stochastic travel times), and (iii) crowding discomfort externalities (with or without considering in-vehicle crowding costs). The benefits of vehicle automation are assessed under different degrees of automation (i.e., human driving costs that can be partially or fully saved depending on automation capabilities). The effects of automation on travel time volatility and dwell time regularity are also studied. Besides, the optimal degrees of increment in frequency and vehicle size, due to the inclusion of crowding externalities and travel time stochasticity, are identified for both types of fleets. In essence, the most prominent contribution of this work stems from the experimentation relevant for automated buses. To achieve this aim, a detailed framework is provided for the formulation of automated bus problems, while considering various components concurrently, such as crowding discomfort externalities and stochastic travel times. Thus, in terms of application-based contributions, such a high-resolution model enables us to perform several experiments under different scenarios for a thorough and wide-ranging assessment of the service and cost implications of the deployment of automated buses.

The main contributions of our work are the following. First, we extensively compare the effects of in-vehicle crowding discomfort on determining the optimal service frequency and vehicle size for a fleet of automated buses vs. a fleet of conventional human-driven buses. While it is expected that frequencies and bus sizes are going to increase for both fleets of human-driven and automated buses if in-vehicle crowding is considered as a source of travel disutility for users, the crucial question arising here is whether these items are increased at a similar rate for both fleets or not. This issue has implications for the optimal design of future public transport systems, for the comfort level that will be delivered to users (in terms of occupancy rates inside vehicles), and for the cost-benefit analysis of public transport investments in crowding-sensitive frameworks. Second, we investigate if the implementation of an automated bus system can decrease the number of left-behind travelers in busy bus routes, due to providing more frequent services at lower operating costs with automation. Third, the effects of travel time uncertainty on the optimal deployment of an automated bus system vs. a human-driven bus system are closely examined, given that the potential provision of more certain travel times is an added benefit of automation in public transport. Finally, to comprehensively evaluate the possible effects of vehicle automation on the social costs of a public transport system, an extensive range of sensitivity analysis tests are performed with alternative assumptions.

The remainder of this paper is organized as follows. Section 2 presents the theoretical and empirical background on passenger crowding and travel time stochasticity in public transportation. In Section 3, a mathematical modeling framework is presented for optimizing service frequency and bus size. In Section 4, a broad range of numerical simulations and sensitivity analysis tests are performed, and the results are extensively interpreted there. Finally, concluding remarks and future research ideas are given in Section 5.

2. Background: Passenger crowding and travel time stochasticity in public transport.

2.1. Crowding in public transport systems: Effects and modeling approaches

Public transport systems in several cities across the globe are experiencing increasing congestion and crowding with the rapid growth of public transportation ridership (Jenelius, 2018). Indeed, public transport crowding can negatively affect users' trip experience and service performance (Drabicki et al., 2020). For instance, crowding phenomena can significantly escalate the discomfort of public transport users inside vehicles (i.e., in-vehicle crowding discomfort), as well as the possibility of denied boardings (Tirachini et al., 2013; Cats et al., 2016; Hörcher and Tirachini, 2021). To simulate realistic operating conditions, only few studies in the literature of automated bus services (e.g., Dai et al., 2020; Hatzenbühler et al., 2020) have considered the possibility of denied boardings. Nonetheless, to the best of our knowledge, an explicit modeling of in-vehicle crowding discomfort (at a microscopic resolution for both sitting and standing travelers) has not yet been included in the optimal design and deployment of automated bus systems. Besides, covering this issue would be more notable in a state-of-the-art model that also contains other aspects of operations explicitly, enabling us to capture crowding discomfort effects together with the concurrent effects of travel time stochasticity and driving cost saving levels with automation on the planning of automated buses.

It has been found that on-board comfort has a profound effect on the satisfaction and loyalty of public transport users (Van Lierop et al., 2018; Soza-Parra et al., 2019). In-vehicle crowding discomfort leads to an increase in the value of in-vehicle time savings (Hörcher et al., 2017). Indeed, the effect of in-vehicle crowding on travel time disutility is typically expressed using an additional in-vehicle travel time multiplier, called crowding multiplier, which increases with the occupancy of vehicles and is larger for standing passengers than for sitting passengers (e.g., Whelan and Crockett, 2009; Wardman and Whelan, 2011; Tirachini et al., 2013, 2017; Jenelius, 2020; Yap et al., 2020).

To optimize public transport frequency and vehicle size in the presence of crowding externalities, the crowding phenomenon is usually included in service supply optimization models through forming a total cost function, in which the user cost is sensitive to in-vehicle crowding levels (Jara-Díaz and Gschwender, 2003; Tirachini et al., 2014; An et al., 2020). For instance, for the determination of optimal frequency and vehicle size, Jara-Díaz and Gschwender (2003) and Tirachini et al. (2014) have highlighted the importance of considering in-vehicle crowding discomfort as a source of disutility for travelers, leading to an increase in frequency and vehicle size compared to the cases in which the user cost is assumed to be insensitive to in-vehicle crowding levels. Likewise, many other studies have so far focused on determining public transport planning decisions while accounting for in-vehicle crowding discomfort, e.g., in frequency and vehicle size determination problems (Batarce et al., 2016; Cats and Glück, 2019; Hörcher and Graham, 2018; Klumpenhouwer and Wirasinghe, 2016; Zhang et al., 2020a); frequency determination problems (Agrawal et al., 2020; Jiang et al., 2014; Pathak et al., 2020; Qin, 2014; Hörcher et al., 2018; Suman and Bolia, 2019; Hörcher et al., 2020); timetabling design methods (Shang et al., 2019); seat provision in public transport (Hörcher et al., 2018; Hamdouch et al., 2011; De Palma et al., 2015).

Besides, for further discussion in this regard, the interested readers are referred to the review paper of Hörcher and Tirachini (2021) who have identified crowding discomfort as an important ingredient in the determination of vehicle size and frequency. An in-depth discussion of in-vehicle discomfort matters is also given in the Transit Cooperative Research Program (TCRP)-165 Report (2013), where the quality of service (QOS) thresholds are also presented and categorized from an on-board comfort perspective (Brinckerhoff, 2013). Overall, the most common way to deal with in-vehicle crowding discomfort is to increase service frequency (Tirachini et al., 2013, 2014; Batarce et al., 2016; Van Lierop et al., 2018).

Regarding implications for cost-benefit analysis, Cats et al. (2016) developed a novel modeling framework considering the dynamics of public transport congestion in the appraisal of large public transport investments. A case study of a metro extension in Stockholm indicated that the benefits gained by the inclusion of dynamic congestion and crowding effects into a cost-benefit analysis can constitute more than a third of the total passenger benefits, and such effects are remarkably underestimated by a static model. Along the same lines, Tirachini et al. (2016) estimated that not accounting for standing externalities in Singapore's East-West MRT line underestimates the disutility of travel time by 28% in the morning peak period. All these findings clearly point to the relevance of crowding externalities for system design and estimation of benefits in public transport project appraisal. Crowding costs are considered in the cost-benefit analysis of transport investments in the United Kingdom, France, Sweden, Australia, New Zealand, and Japan (ITF/OECD, 2014).

2.2. Stochastic nature of public transport operations: Effects of travel time stochasticity

One of the main sources of instability in urban bus operations is the variations of vehicle travel times between stops, caused by a wide range of external factors, such as traffic congestion, traffic lights, weather, and human driving behavior (Muñoz et al., 2020). In this context, several scholars have employed log-normal distribution to model stochastic running times of buses (e.g., Hickman 2001; Zhao et al., 2003; Cats et al., 2011; Delgado et al., 2012; Sánchez-Martínez et al., 2016; Dai et al., 2019; Dai et al., 2020).

The explicit inclusion of travel time stochasticity into the frequency setting problem of automated buses is another incremental contribution to the automated bus literature. As the closest relevant study in relation to this subject, accounting for stochastic travel times, we refer to Dai et al. (2020). Nonetheless, compared to our study, a different scheduling problem with a mixed bus operating environment has been addressed in Dai et al. (2020), focusing on real-time dispatching of automated buses with varying capacities among human-driven buses to provide a more flexible capacity solution to passenger demand fluctuations. Besides, fleet size determination, vehicle capital costs, human driving cost savings with automation, and crowding discomfort effects have not been considered in their study.

Table 1
List of notations.

Symbol	Description	Unit
Sets		
V	Set of buses, V $= \{1, 2, \cdots, N_v\}$	
S	Set of stops,$S = \{1, 2, \cdots, N_s\}$	
Indices		
i	Index of buses	
j, k	Index of stops (from origin j to destination k)	
Input parameters		
N_s	Number of stops on the route	
R	Route length	km
$\lambda_j[t]$	Passenger arrival rate at stop j at time t	pax/min
$OD_{j,k}[t]$	Destination distribution matrix (the percentage of passengers at stop j, who aim to travel from stop j to stop k, $k > j$) at time t	%
$f_{\min}$	Minimum frequency	veh/h
$f_{\max}$	Maximum frequency	veh/h
T	Start of the study period	min
δ_a	Acceleration time	s
δ_d	Deceleration time	s
τ	Time required for opening and closing bus doors	s
T_c	Cycle time	min
α_a	Average alighting time per passenger	s/pax
α_b	Average boarding time per passenger	s/pax
P_a	Proportion of passengers alighting through the busiest door of a bus	%
P_b	Proportion of passengers boarding through the busiest door of a bus	%
h	Dispatching headway from the first stop	min
φ^{w1}	Monetary value of initial waiting time	€/h
φ^{w2}	Monetary value of extra waiting time due to denied boarding	€/h
φ^{v}	Monetary value of in-vehicle travel time	€/h
φ^{d}	Hourly driving cost	€/veh-h
φ^{run}	Running cost of a vehicle per kilometer	€/veh-km
φ^{cap}	Capital cost of a vehicle per hour, i.e., cost of owning or renting a vehicle per hour	€/veh-h
ω	Driving cost coefficient for reflecting the level of reduction in human driving costs due to automation	
β	Capital cost coefficient for reflecting the level of increase in vehicle capital costs due to automation	
θ	Running cost coefficient for reflecting the level of reduction in vehicle running costs due to automation	
α^{sit}	Seated in-vehicle time multiplier	
α^{stand}	Standing in-vehicle time multiplier	
$C(v_s)$	Total capacity of a vehicle, which is a function of the vehicle size	pax/veh
$n^{\text{seat}}(v_s)$	Number of seats inside a vehicle, which is a function of the vehicle size	
Auxiliary variables		
N_v	Fleet size	veh
$T^a_{i,j}$	Arrival time of bus i at stop j	min
$T^d_{i,j}$	Departure time of bus i from stop j	min
$T^s_{i,j}$	Dwell time of bus i at stop j	min
$T^r_{i,j}$	Running time of bus i between stops $j-1$ and j	min
$H_{i,j}$	Headway between buses $i-1$ and i at stop j	min
$N^c_{i,j,k}$	Number of passengers with trip $j \to k$ arriving at stop j during the headway between buses $i-1$ and i	pax
$N^f_{i,j,k}$	Number of passengers with trip $j \to k$ failing to board bus i at stop j	pax
$N^w_{i,j,k}$	Number of passengers with trip $j \to k$ waiting for bus i at stop j	pax
$N^c_{i,j}$	Total number of passengers arriving at stop j during the headway between buses $i-1$ and i	pax
$N^f_{i,j}$	Total number of passengers failing to board bus i at stop j	pax
$N^w_{i,j}$	Total number of passengers waiting for bus i at stop j	pax
$N^{on}_{i,j}$	Number of passengers inside bus i between stops $j-1$ and j	pax
$N^{\text{sit}}_{i,j}$	Number of seated passengers inside bus i between stops $j-1$ and j	pax
$N^{\text{stand}}_{i,j}$	Number of standing passengers inside bus i between stops $j-1$ and j	pax
$F_{i,j}$	Load factor of bus i between stops $j-1$ and j	pax/seat
$N^b_{i,j}$	Number of passengers boarding bus i at stop j	pax
$N^a_{i,j}$	Number of passengers alighting bus i at stop j	pax
$N^s_{i,j,k}$	Number of passengers with trip $j \to k$, who can successfully board bus i at stop j	pax
Decision variables		
f	Service frequency (Allowed frequency values: $f \in \underbrace{\{f_{min}, f_{min}+1, \ldots, f_{max}-1, f_{max}\}}_{\text{discrete set with } (f_{max}-f_{min})+1 \text{ elements}}$)	veh/h
v_s	Vehicle size (four bus sizes used as candidates: $v_s \in \{8,\ 12,\ 15,\ 18\}$ meters)	m

"pax" stands for passenger.
"min" stands for minute.

Unreliable travel times have a negative impact on passenger waiting time at stops (Durán-Hormazábal and Tirachini, 2016). In addition, although waiting time affects overall user satisfaction (Tyrinopoulos and Antoniou, 2008; Dell'Olio et al., 2011), waiting time due to unreliability (e.g., travel time uncertainty) has deeper negative consequences on users' satisfaction (Rietveld et al., 2001; Van Lierop et al., 2018). Hence, unexpected waiting delays associated with unreliable services can substantially degrade the attractiveness of a public transport system. On the other hand, the differences in human driving functions, which can introduce considerable uncertainty in travel time during real-world operations (Wang and Sun, 2020), can be much less pronounced in the operation with automated vehicles due to the elimination of distracted driving and bad driving behavior (Azad et al., 2019). Moreover, Dai et al. (2020) assume that automated buses can dynamically and accurately adjust their running times given the forward and backward headways thanks to automation capabilities, thus making automated bus systems more robust to random disruptions. Nonetheless, it is worth noting that the public acceptance of driverless bus systems can be affected by users' perceptions about the security and safety of such systems in real-world operations. For example, the findings of the current stage of automated bus programs show that there is still a propensity for the use of human-driven buses for trips longer than few minutes, as there are still some concerns about the operational safety of automated buses among users, especially in mixed traffic environments (Salonen, 2018; Dong et al., 2019; Nemoto et al., 2020).

Driving time volatility between stops can also lead to a further growth of irregularity in dwell times of vehicles at stops due to poor service reliability, early or late services (van Oort, 2014), i.e., travel time variations have adverse effects on dwell time regularity at stops. Nonetheless, this aspect has still not been studied in the deployment of a fleet of automated vehicles that might be operated with different travel time variation levels. The possible influences of automation on travel time volatility, and dwell time regularity are extensively examined in this study.

3. Model formulation

We develop a mathematical modeling framework for solving the problem of setting service frequency and vehicle size for fleets of human-driven or automated buses. To this end, we formulate a comprehensive objective function, which calculates both user and operator costs, to minimize the total costs of a public transport service in the presence of crowding externalities, time-dependent demand flows, and stochastic travel times. Besides, several constraints are modeled to represent real-world operating conditions, such as vehicle movement, passenger flow, and vehicle capacity restrictions in line with the remaining on-board capacity of vehicles during operations. Table 1 includes the notations employed in our problem formulation.

3.1. Model assumptions

The main assumptions employed in our problem formulation are listed as follows:

- We consider high-frequency bus systems, where the arrivals of passengers at stations are assumed to be random.
- We consider 15-minute-dependent demand volumes, remaining fixed during each 15-minute interval (every 15 min).
- We consider a general bi-directional bus corridor with even dispatching headways from the first stop.
- We model varying dwell times (flow-dependent dwell times), which can vary for a vehicle at each stop as a function of the number of passengers getting off and on at that stop.
- We assume a log-normal distribution for stochastic running times between stops.
- We consider vehicle capacity restrictions, and hence:
  (a) boarding numbers will never exceed the residual capacity inside vehicles;
  (b) extra waiting times are considered for denied boarding situations;
  (c) when boarding demand is larger than the residual capacity inside a bus, the chance of boarding is assumed to be the same for all the travelers waiting for that bus, independent of their trip destinations[1].
- We assume that overtaking is not permitted during bus operations.
- For user cost calculations, we distinguish between the monetary values of in-vehicle travel time, initial waiting time, and extra waiting time due to denied boarding.
- We estimate passenger occupancy rates, the number of seated and standing passengers inside vehicles, and crowding discomfort at a microscopic level, bus by bus.
- We assume that the user cost is sensitive to on-board crowding levels, i.e., the impacts of on-board crowding on the disutility of in-vehicle travel time for both seated and standing passengers are modeled.
- We assume that the technology of automation can:
  (a) increase vehicle capital costs due to including automation technologies inside vehicles;
  (b) reduce human driving costs;
  (c) reduce vehicle running costs through a reduction in fuel/energy consumption due to providing a more balanced driving style.

[1] This is a common assumption that has been employed by several studies in the literature (e.g., Wang et al., 2015; Gao et al., 2016; Sánchez-Martínez et al., 2016; Dai et al., 2020; Sadrani et al., 2022).

3.2. Objective function

The objective function (1) minimizes the total cost of a public transport service, defined as the sum of user and operator costs. User cost (Z_p) is composed of two components: waiting and in-vehicle time costs. Operator cost (Z_o) is comprised of three components: capital, driver, and running costs. A single-objective optimization model allows for establishing a trade-off between user and operator costs simultaneously, thus finding the optimal solution that leads to the minimum total cost (social cost) of a public transportation service. In the present research, we employ various monetary valuations[2] to translate all travel time/distance elements which are relevant to passengers and operators into their equivalent cost values. Further details are provided on each monetary term in the following.

It has been shown that the value of waiting time at stops is larger than the value of in-vehicle time (Wardman, 2004; Cats et al., 2016; Lu et al., 2018). Moreover, the value of extra waiting time due to denied boarding (for passengers left behind due to capacity constraints) is larger than the value of initial waiting time experienced in normal cases (Cats et al., 2016; Cats and Jenelius, 2018). For instance, Cats et al. (2016) assumed that one minute waiting time after being denied boarding is perceived 3.5 times as onerous as one minute initial waiting time. Accordingly, using three different monetary valuations, namely φ^{w1}, φ^{w2}, and φ^{v} [€/h], we distinguish between the monetary values of initial waiting time, extra waiting time caused by denied boarding, and in-vehicle time.

For operator cost estimations, vehicle capital costs and driver costs are commonly defined on a temporal basis [€/veh-h or €/veh-day], whereas running costs are defined on a spatial basis [€/veh-km] (Tirachini and Antoniou, 2020). Hence, in our setting, φ^{d} and φ^{cap} [€/veh-h] are used to convert vehicle operating hours into driver and vehicle capital costs respectively, whereas φ^{run} [€/veh-km] is used to translate the distance traveled by vehicles into their running costs.

$$Z = \underbrace{Z_{\text{w}} + Z_{v}}_{Z_p} + \underbrace{Z_{\text{cap}} + Z_{\text{driver}} + Z_{\text{run}}}_{Z_o} \tag{1}$$

Considering the objective function (1) and the problem constraints, which will be given in Section 3.3, the master problem for the joint optimization of service frequency (f) and vehicle size (v_s) is presented as follows:

$$\text{Master Problem} \begin{cases} \underset{f, v_s}{\text{Min}}\ Z \\ \text{Subject to constraints (12) - (32)} \end{cases} \tag{2}$$

3.2.1. User cost

As indicated in expression (3), the total waiting time cost accounts for: (i) initial waiting time costs for new passengers entering stops during the headway, plus (ii) extra waiting time costs due to denied boarding considered for left-behind passengers, who could not board the earlier bus due to crowding.

Buses run frequently enough in high-frequency bus systems, and thus passengers do not need to coordinate their arrivals with the arrival times of vehicles, i.e., we assume random arrivals at stations. Accordingly, the average waiting time is estimated as half of the headway ($H_{i,j}/2$) for travelers in group (i) [see Eq. (4)], in line with a common assumption in this field (e.g., Furth and Wilson, 1981; Wu et al., 2017; Gkiotsalitis and Cats, 2018; Dai et al., 2020; Sadrani et al., 2022). However, the extra waiting time is the entire headway ($H_{i,j}$) for travelers in group (ii), who must wait for the next vehicle [see Eq. (5)]. Given the higher value of extra waiting time (φ^{w2}) than that of initial waiting time (φ^{w1}), denied boardings can lead to a remarkable increase in passengers' waiting time costs.

$$Z_w = Z_w^{(i)} + Z_w^{(ii)} \tag{3}$$

$$Z_w^{(i)} = \varphi^{w1} \sum_{i \in V} \sum_{j \in S} N_{i,j}^{c} \cdot \frac{H_{i,j}}{2} \tag{4}$$

$$Z_w^{(ii)} = \varphi^{w2} \sum_{i \in V, i \geqslant 2} \sum_{j \in S} N_{i-1,j}^{f} \cdot H_{i,j} \tag{5}$$

The cost of passengers' in-vehicle time has two components: the cost of riding time between stops, i.e., $Z_{\text{v}}^{\text{ride}}$, as well as the cost of dwell time at stops, i.e., $Z_{\text{v}}^{\text{dwell}}$.

$$Z_v = Z_v^{\text{ride}} + Z_v^{\text{dwell}} \tag{6}$$

$$Z_v^{\text{ride}} = \varphi^{v} \sum_{i \in V} \sum_{j \in S, j \geqslant 2} \left(T_{i,j}^{r} + \delta_{\text{a}} + \delta_{d} \right) \cdot \left(\alpha^{\text{sit}}\ N_{i,j}^{\text{sit}} + \alpha^{\text{stand}}\ N_{i,j}^{\text{stand}} \right) \tag{7}$$

$$Z_v^{\text{dwell}} = \varphi^{v} \sum_{i \in V} \sum_{j \in S, j \geqslant 2} \left(N_{i,j}^{on} - N_{i,j}^{a} \right) \cdot T_{i,j}^{\text{v}} \tag{8}$$

[2] φ^{w1} [€/h], φ^{w2} [€/h], and φ^{v} [€/h] are used for user cost calculations. Moreover, φ^{cap} [€/veh-h],φ^{d} [€/veh-h], and φ^{run} [€/veh-km] are used for operator cost calculations.

As presented in expression (7), the cost of riding time between stops is obtained through multiplying the total number of on-board passengers (including both seated and standing passengers) by the total time required for traveling between each two successive stops. Besides, the user cost is sensitive to in-vehicle crowding levels in this formulation, which enables us to estimate in-vehicle discomfort costs for passengers depending on occupancy levels inside each vehicle at each segment of the route. Indeed, in-vehicle crowding has been found as a significant source of travel disutility for both seated and standing passengers, thereby increasing perceived in-vehicle times for both groups of travelers. Following Wardman and Whelan (2011), we draw a distinction between the value of in-vehicle time for seated and standing passengers through employing crowding multipliers of α^{sit} and α^{stand} respectively. As indicated in Table 2[3], crowding multipliers increase with the growth of the load factor and are larger for standing passengers than for seated passengers. For instance, to estimate the user cost of crowding, when the passenger load factor is 110%, the perceived in-vehicle time is increased to [1.05 × (actual in-vehicle time)] for seated passengers, whereas it is increased to [1.62 × (actual in-vehicle time)] for standees. In our numerical experiments, we will widely examine the influences of on-board crowding and standing on determining the optimal service frequency and vehicle size for a fleet of automated buses vs. human-driven buses.

As can be seen in (8), Z_v^{dwell} is related to those passengers, $N_{i,j}^{on} - N_{i,j}^{a}$, inside bus i whose destination is not bus stop j (i.e., they do not need to alight at stop j), so they have to stay inside bus i during alighting and boarding times (dwell time) at that stop.

3.2.2. Operator cost

Operator cost elements, incorporated into the objective function (1), are described here. Vehicle automation can potentially affect operator costs in three aspects: a rise in capital cost, and reduction in driver and running costs. Following Tirachini and Antoniou (2020), we formulate operator costs in a general manner for human-driven bus operations, and the effects of vehicle automation on operator costs (including capital, driver, and running costs) are separately described by additional factors, namely β ($\beta \geq 1$), ω ($0 \leq \omega \leq 1$), and θ ($0 \leq \theta \leq 1$). Obviously, for human-driven bus operations in our framework, such factors would be equivalent to one.

The total vehicle capital cost (fleet acquisition cost) is estimated by Eq. (9).

$$Z_{\text{cap}} = \beta\ \varphi^{\text{cap}} \sum_{i \in V} \sum_{j \in S_i, j \geqslant 2} \left(T_{i,j}^{s} + T_{i,j}^{r} + \delta_{\text{a}} + \delta_{d} \right) \tag{9}$$

For automated bus fleets, coefficient β ($\beta \geq 1$) represents the level of increase in vehicle capital costs due to including automation technologies in vehicles, e.g., $\beta = 1.5$ indicates an increase of 50% in vehicle capital costs with automation. This parameter value has been estimated by Tirachini and Antoniou (2020) for different vehicle sizes.

The total driving cost is estimated by Eq. (10).

$$Z_{\text{driver}} = \omega\ \varphi^{d} \sum_{i \in V} \sum_{j \in S_i, j \geqslant 2} \left(T_{i,j}^{s} + T_{i,j}^{r} + \delta_{\text{a}} + \delta_{d} \right) \tag{10}$$

It is not expected that the technology of automation can totally eliminate human-related driven costs, as some employees are still retained to control or monitor the operation of bus routes with automated driving technologies, provide information to users, and safeguard the security of operations and passengers, among other new needs of personnel that may arise in an automated public transport system (Abe, 2019; Tirachini and Antoniou, 2020). Hence, for automated fleets, coefficient ω ($0 \leq \omega \leq 1$) reflects the level of current human driving costs being needed after automation. For example, $\omega = 0$ shows the case of full driving cost savings with automation, whereas $\omega = 0.6$ shows that 40% of salaries are saved with automation.

Eq. (11) accounts for the total running cost (e.g., energy consumption, tires, maintenance) based on the total distance traveled by vehicles.

$$Z_{\text{run}} = \theta\ .\ \varphi^{run}.\ R\ .\ N_{v} \tag{11}$$

Coefficient θ ($0 \leq \theta \leq 1$) represents the level of reduction in running costs with automated vehicles, which can reduce fuel/energy consumption per veh-km due to providing more balanced driving functions thanks to, e.g., V2V and V2I communications (Wadud, 2017; Bösch et al., 2018; Tirachini and Antoniou, 2020). For example, $\theta = 0.9$ means that 10% of vehicle running costs per kilometer can be saved with automation.

3.3. Constraints

In this part, we model vehicle motion constraints, as well as passenger flow constraints acting in accordance with the available capacity of vehicles during operations (i.e., the possibility of denied boarding due to a shortage of capacity). Overall, a bus movement model includes the calculations of five key elements: arrival times at stops, departure times from stops, headways between consecutive vehicles, dwell times at stops, and running times between successive stops. Furthermore, our passenger flow constraints include the calculations of six components: the number of passengers waiting at stops, the number of seated/standing passengers inside vehicles, the number of passengers who can/cannot successfully board vehicles, and the number of passengers alighting at stops.

[3] The values presented in Table 2 have been taken from the *meta*-study of Wardman and Whelan (2011).

3.3.1. Vehicle movement constraints

The service frequency is regarded as a decision variable, which can be chosen from a discrete set of values subject to predefined lower and upper bounds of $f_{\min}$, and $f_{\max}$ [veh/h], i.e.,

$$f \in \{f_{\min},\ f_{\min}+1,\ \ldots,\ f_{\max}-1,\ f_{\max}\} \tag{12}$$

In general, $f_{\min}$ is often given by a minimum capacity (or maximum waiting time) that is exogenously defined in public transport systems. As mentioned in the model assumptions, we focus on high-frequency bus services, where buses run frequently enough so that passengers do not need to coordinate their arrivals with bus arrivals. In this regard, some studies in the literature have considered high-frequency service as services operating with a frequency of at least 5 [veh/h] or more (e.g., Bartholdi and Eisenstein, 2012; Chiraphadhanakul and Barnhart, 2013; Gkiotsalitis and Van Berkum, 2020a). On the other hand, $f_{\max}$ is given by the capacity of bus stops (Tirachini, 2014).

The fleet size requirement is obtained as follows:

$$N_v = [f.T_c] \tag{13}$$

where T_c represents the total travel time during one cycle or round-trip (Tirachini et al., 2014).

Headway between vehicles $i-1$ and i at stop j is obtained as follows:

$$H_{i,j} = T^d_{i,j} - T^d_{i-1,j} \quad \forall i \in V - \{1\}, \forall j \in S \tag{14}$$

As can be seen in (15), the arrival time of bus i at stop j is obtained through the sum of: (1) the departure time of bus i from stop $j-1$, (2) acceleration time for leaving stop $j-1$, (3) the running time between stops $j-1$ and j, and (4) deceleration time for entering stop j.

$$T^a_{i,j} = T^d_{i,j-1} + \delta_a + T^r_{i,j} + \delta_d \quad \forall i \in V, \forall j \in S - \{1\} \tag{15}$$

Running times are stochastic, drawn from a log-normal distribution:

$$T^r_{i,j} \sim \text{log}normal\ (r_j,\ \sigma_j) \quad \forall i \in V, \forall j \in S - \{1\} \tag{16}$$

where r_j and σ_j represent respectively the mean and standard deviation of running time between stops $j-1$ and j. In our numerical experiments, we perform a sensitivity analysis on travel time variability for automated vehicle fleet operations with changes in the standard deviation of travel times.

It is assumed that vehicles are dispatched at even dispatching headways from the first stop. As indicated in Eq. (17), an even interval of h minutes ($h = 60/f$) is considered between the dispatching of vehicles, e.g., for a frequency of 20 (veh/h), buses are dispatched every 3 min from the first stop. Besides, we assume that the first bus is dispatched at a certain time which is the beginning of the study period (T) (i.e., the departure time of the first bus from the first stop is set to the first time point).

$$T^d_{i,1} = T + \quad (i-1)h \quad \forall i \in V \tag{17}$$

At other bus stops, the departure time of bus i at stop j is obtained by adding its dwell time to its arrival time at stop j, as presented in Eq. (18).

$$T^d_{i,j} = T^a_{i,j} + T^s_{i,j} \quad \forall i \in V, \forall j \in S - \{1\} \tag{18}$$

We model flow-dependent dwell times. Regarding the alighting and boarding policy, we assume that passengers use the same doors for alighting and boarding, and that the boarding process will always begin after finishing the alighting process (i.e., sequential alighting and boarding, in which the alighting process has priority over the boarding process). Hence, the total dwell time at a stop depends on the sum of the passengers' alighting and boarding times (Tirachini et al., 2014). As presented in Eq. (19), the dwell time of bus i at stop j depends on the number of passengers getting off and on through the busiest bus door, plus a fixed "dead" time spent opening and closing bus doors.

$$T^s_{i,j} = \tau + P_a \alpha_a N^a_{i,j} + P_b \alpha_b N^b_{i,j} \quad \forall i \in V, \forall j \in S \tag{19}$$

Parameters P_a and P_b represent respectively the proportions of passengers alighting and boarding through the busiest door of a bus, and are dependent on the number of bus doors (note that the values of such size-dependent parameters are given in Tables A2 and A3 in Appendix A) (Tirachini et al., 2014). Parameters α_a and α_b represent the average alighting and boarding times per passenger respectively, and depend on fare payment methods, bus floor height, platform configuration, and so on. Another relevant aspect to explain here is the effects of active vehicle capacity constraints on dwell times. Indeed, since we explicitly account for vehicle capacity constraints, the dwell times of vehicles (in terms of boarding time) can depend on the remaining capacity of vehicles at each stop (the boarding numbers, $N^b_{i,j}$ in Eq. (29), cannot exceed the remaining capacity). Moreover, in our numerical studies, we carry out a sensitivity analysis on the dead time (τ) to evaluate the possible effects of vehicle automation on the process of opening and closing bus doors.

3.3.2. Passenger flow constraints

Given time-dependent demand volumes, Eq. (20) calculates the number of passengers arriving at origin stop j over the headway,

who wait for the arrival of bus i to travel from stop j to stop k (trip $j \rightarrow k$).

$$N^{c}_{i,j,k} = \int_{T^{d}_{i-1,j}}^{T^{d}_{i,j}} \lambda_j[t].\ OD_{j,k}[t].\ dt \quad \forall i \in V, \forall j, k \in S, k > j \tag{20}$$

Following Gao et al. (2016) and Sadrani et al. (2022), we use 15-minute-dependent demand data, remaining fixed during each 15-minute interval. For an in-depth discussion of fine-grained demand information and demand aggregation intervals under different degrees of demand availability for public transport planning, we refer to Sadrani et al. (2022). In this regard, the authors have examined and compared the effects of demand data resolution on the accuracy of waiting time estimations. Hence, 15-minute-dependent demand data are introduced as fine-grained demand information that can suitably capture passenger demand variations for planning purposes.

Considering passengers left behind by the earlier bus (i.e., bus $i-1$) at stop j, the total number of passengers with trip $j \rightarrow k$ waiting for bus i at stop j includes two groups of passengers [see Eq. (21)]: (i) the new passengers arriving at stops during the headway, modeled in Eq. (20), and (ii) those passengers previously left behind.

$$N^{w}_{i,j,k} = N^{c}_{i,j,k} + N^{f}_{i-1,j,k} \quad \forall i \in V, \forall j, k \in S, k > j \tag{21}$$

According to the above-mentioned definitions, it is evident that Eqs. (22)-(24) will always hold. For instance, passengers waiting for bus i at stop j can have various trip destinations. Hence, given the definitions of $N^{w}_{i,j,k}$ and $N^{w}_{i,j}$, to calculate the total number of passengers waiting for bus i at stop j, all the waiting passengers at that stop with any trip destinations (trip $j \rightarrow k$, $k > j$) are summed together using Eq. (24).

$$N^{c}_{i,j} = \sum_{k \in S, k > j} N^{c}_{i,j,k} \quad \forall i \in V, \forall j \in S \tag{22}$$

$$N^{f}_{i,j} = \sum_{k \in S, k > j} N^{f}_{i,j,k} \quad \forall i \in V, \forall j \in S \tag{23}$$

$$N^{w}_{i,j} = \sum_{k \in S, k > j} N^{w}_{i,j,k} \quad \forall i \in V, \forall j \in S \tag{24}$$

As shown in Eq. (25), the number of on-board passengers of bus i between stops $j-1$ and j, N^{on}_{ij}, includes those passengers who have remained on bus i from the earlier segment ($j-2 \rightarrow j-1$) as they do not need to alight at stop $j-1$, i.e., ($N^{on}_{i,j-1} - N^{a}_{i,j-1}$), plus passengers getting on bus i at stop $j-1$, denoted by $N^{b}_{i,j-1}$. Note that vehicles are empty when reaching the first stop (i.e., $N^{on}_{i,1} = 0, \forall i \in V$).

$$N^{on}_{i,j} = N^{on}_{i,j-1} - N^{a}_{i,j-1} + N^{b}_{i,j-1} \quad \forall i \in V, \forall j \in S - \{1\} \tag{25}$$

The number of seated passengers on bus i between stops $j-1$ and j is equal to the minimum value between the number of seats and the number of passengers inside bus i, i.e.,

$$N^{\text{sit}}_{i,j} = \min \left\{ n^{\text{seat}}(v_s),\ N^{on}_{i,j} \right\} \quad \forall i \in V, \forall j \in S \tag{26}$$

The number of standees inside bus i between stops $j-1$ and j is obtained through (27).

$$N^{\text{stand}}_{i,j} = \max \left\{ 0,\ N^{on}_{i,j} - n^{\text{seat}}(v_s) \right\} \quad \forall i \in V, \forall j \in S \tag{27}$$

Load factor $F_{i,j}$, defined as the ratio between the number of on-board passengers and the total number of bus seats, reflects the degree of occupancy inside bus i when traveling between stops $j-1$ and j. High load factors are related to crowding externalities inside vehicles (Wardman and Whelan, 2011; Tirachini et al., 2013).

$$F_{i,j} = \frac{N^{on}_{i,j}}{n^{\text{seat}}(v_s)} \quad \forall i \in V, \forall j \in S \tag{28}$$

The number of passengers who are able to board bus i at stop j will never exceed the residual capacity of bus i at that stop, i.e.,

$$N^{b}_{i,j} = \min \left\{ N^{w}_{i,j},\ C(v_s) - N^{on}_{i,j} + N^{a}_{i,j} \right\} \quad \forall i \in V, \forall j \in S \tag{29}$$

As can be seen in (30), the alighting demand for bus i at stop j will include those passengers boarding bus i at the previous stops, aiming to reach stop j. Note that the alighting demand is zero at the first stop (i.e., $N^{a}_{i,1} = 0, \forall i \in V$).

$$N^{a}_{i,j} = \sum_{j' \in S, j' < j} N^{s}_{i,j',j} \quad \forall i \in V, \forall j \in S - \{1\} \tag{30}$$

As explained before, when capacity is not sufficient to meet the whole boarding demand, we consider the same chance of boarding for all passengers, as modeled in Eq. (31).

$$N^{s}_{i,j,k} = \frac{N^{b}_{i,j}}{N^{w}_{i,j}} N^{w}_{i,j,k} \quad \forall i \in V, \forall j,k \in S, k > j \tag{31}$$

Finally, in Eq. (32), we calculate the number of passengers with trip $j \rightarrow k$, who are unable to board bus i at stop j due to crowding.

$$N^{f}_{i,j,k} = N^{w}_{i,j,k} - N^{s}_{i,j,k} \quad \forall i \in V, \forall j,k \in S, k > j \tag{32}$$

4. Numerical experiments and application

4.1. Scenario setting and input data

To examine the applicability of the proposed mathematical model, an extensive range of scenarios are simulated for two real-world bus corridors in the cities of Regensburg in Germany and Santiago in Chile, averagely serving the total hourly demand of 638 [pax/h] and 5764 [pax/h] respectively during the morning rush hours. Regarding the analysis period, our simulations are conducted for a two-hour period extending from 7:00 to 9:00 AM. Time-dependent demand data related to the entire simulation period are presented in Appendix A (Table A4). The Regensburg case study is Bus Line 1 in the Konradsiedlung in Pommernstr, and the Santiago case study is Los Pajaritos corridor with bus passenger demand taken from Cortés et al. (2011). Both bus routes are bi-directional, containing a total number of 24 bus stops (12 stops in each direction) in Regensburg and 20 bus stops (10 stops in each direction) in Santiago.

Input parameters used in the base case scenarios are presented in Appendix A (see Tables A1-A3). All the cost parameters for both Germany and Chile are based on electric vehicles for both human-driven and automated public transport operations, and were estimated by Tirachini and Antoniou (2020). It should be noted that we focus on a homogeneous fleet of buses (the fleet is composed of buses of the same size), and therefore size-dependent parameters (listed in Tables A2 and A3 for Regensburg and Santiago respectively) are not changed from one service to another, depending on the size of each service. In essence, such items are simply initialized (in the step of parameters' initialization) based on the (fixed) vehicle size assigned to our homogeneous fleet operation, and remain fixed during the entire simulation time for that fleet (note that the parameter initialization step is described further when presenting the main steps of the solution approach in subsection 4.2). Hence, we are not confronted with a particular difficulty in handling those parameters (e.g., in the objective function) during the simulation period. By contrast, this can be indeed a complicated issue in mixed/heterogeneous fleet problems (i.e., when buses of different sizes are operated). In this case, additional constraints and steps should be designed to handle the error and computational complexity of varying parameters, which can continuously vary from one service to another during operations.

Considering automated and human-driven vehicles, deterministic and stochastic travel times, and the presence or absence of in-vehicle crowding effects, a total of 8 different combinations of scenarios are simulated, as listed in Table 3. The optimal frequency and vehicle size are determined for any given scenario in both case studies of Regensburg and Santiago. Moreover, to comprehensively evaluate the possible effects of vehicle automation on the social costs of public transport services, several tests of sensitivity are performed on human driving cost savings with automation, travel time stochasticity, dwell time regularity, the time lost to open and close bus doors with automation, crowding multipliers, extra waiting time values, and user- and operator-oriented design cases.

4.2. Solution approach

As discussed in the mathematical formulation, variables of service frequency and vehicle size, confined to the predetermined discrete sets of $\{f_{\min}, f_{\min}+1, \cdots, f_{\max}-1, f_{\max}\}$ [veh/h] and {8,12,15,18} [meters] respectively, are considered as the decision variables in our model. As for vehicle sizes, our range goes from minibuses and standard 12-m long buses, to articulated 18-m long buses. Due to the combinatorial nature of the problem, there is a limited number of possible solutions that need to be evaluated in each scenario (with a full enumeration (exhaustive search) of the solution space) for exploring the whole solution space and finding the global optimal solution leading to the minimum total cost. For instance, for our experiments in Regensburg, $f_{\min}$ and $f_{\max}$ are set to be 5 and 40 respectively, i.e., the set of frequencies is regarded as {5, 6, 7, …, 38, 39, 40} [veh/h], containing a total of 36 elements. Thus, in the presence of 4 different bus sizes used as candidates, there are a total of $36 \times 4 = 144$ possible solutions for exploring the entire solution space using a full enumeration (FL) method. For the given bus route in Santiago, taken as the illustrative example of a corridor with a large volume of passengers [5764 pax/h], $f_{\min}$ and $f_{\max}$ are set to be 15 and 120 [veh/h] respectively. Hence, the total number of possible solutions that should be assessed would be $106 \times 4 = 424$.

It is worth noting that the full enumeration method is a widely-used method in the relevant literature to solve bus scheduling design problems taking advantage of relatively small-scale instances in bus lines (e.g., Fu et al., 2003; Sun and Hickman, 2005; Gkiotsalitis and Cats, 2018; Gkiotsalitis, 2020; Hatzenbühler et al., 2020; Sadrani et al., 2022). Indeed, this exact method is able to return a globally optimal solution (within an acceptable time for relatively small instances), compared to metaheuristics that cannot guarantee the optimality of the solutions. In essence, the solution quality (e.g., finding the global optimal solution) is more important than the saving of computational time when solving such offline design problems (Sadrani et al., 2022), where problems are generally solved once without a hard time pressure to prescribe medium or long-term decisions in the context of important financial investments (Talbi, 2009; Sadrani et al., 2022). That is, computational time saving is not the major issue for policymakers and practitioners in such design problems. Hence, if it is possible, the exact methods should be preferred rather than *meta*-heuristic algorithms that are not able to guarantee the global optimality.

To further describe the proposed full enumeration (FE) method employed to solve our mathematical programming model in Eq. (2),

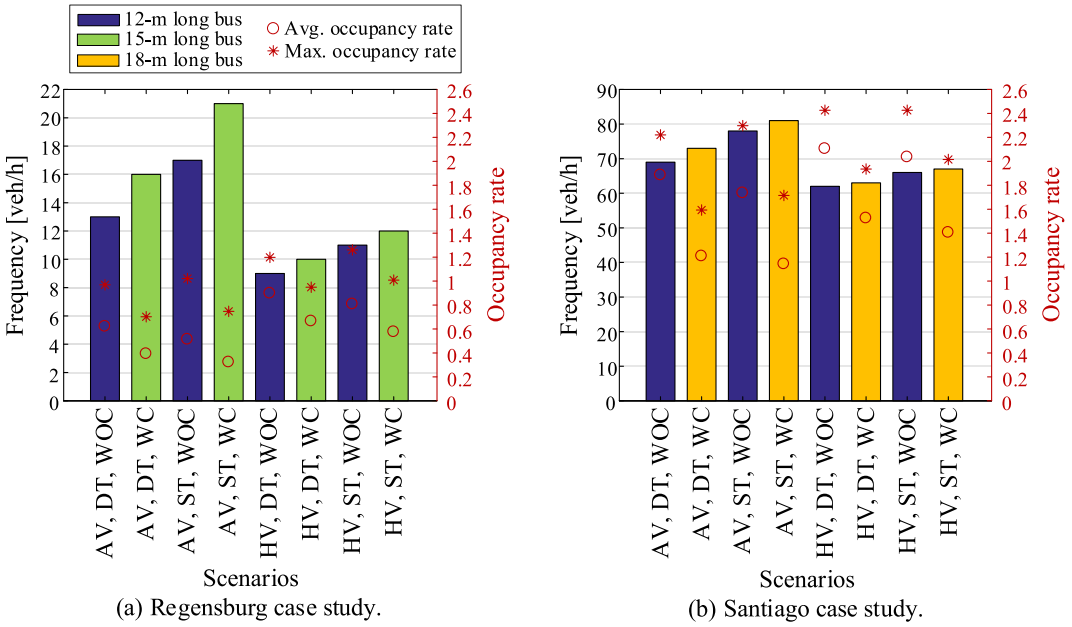

Fig. 1. Optimal service frequency and vehicle size for different scenarios.

the main steps of the FE method are described in Algorithm 1 in Appendix B. Besides, to manage travel time stochasticity in ST scenarios, we utilize a Monte Carlo Simulation (MCS) approach, allowing for the evaluation of each possible solution within multiple repetitions (Liu et al., 2013; Wu et al., 2017; Mou et al., 2020; Zhang et al., 2020b; Gkiotsalitis and Van Berkum, 2020b; Sadrani et al., 2022). In essence, the MCS is activated in the form of a subroutine in the proposed FE algorithm. That is, whenever the FE algorithm needs to do an evaluation process, this task is undertaken by the MCS method (for more details, see Algorithm 2 in Appendix B). The number of MCS runs is set to be 1000 in our study.

Our model is coded in MATLAB R2019b, and all experiments are executed on a personal computer with Intel(R) Core(TM) i5-6500 CPU @ 3.20 GHz and 16.0 GB RAM. For Santiago encompassing more possible solutions to be evaluated compared to Regensburg, the enumeration method can averagely evaluate all the possible solutions within 3.32 min for scenarios assuming deterministic travel times. This is indeed an acceptable computing time for the enumeration of all solutions in an offline design problem. This average amount of time increases to 14.24 min for scenarios with stochastic travel times, due to the run of a MCS scheme for assessing each possible solution over several (1000) replications.

4.3. Optimal service frequency and vehicle size in base case scenarios

In the base case, we assume 50% human driving cost savings due to automation. Results on optimal frequencies and vehicle length are shown in Fig. 1 for Regensburg (1.a) and Santiago (1.b). Furthermore, Fig. 1 gives information on occupancy levels inside vehicles in terms of the average and maximum occupancy rates for any given scenario. Overall, we obtain that fleets of automated vehicles are dispatched with a higher optimal service frequency compared to conventional human-driven services, which is a known result for the case without crowding externalities and deterministic travel times (Fielbaum, 2019; Zhang et al., 2019; Hatzenbühler et al., 2020; Tirachini and Antoniou, 2020). Vehicles are dispatched at a higher frequency in the case of Santiago, in which the total demand volume (5764 [pax/h]) is far larger than Regensburg with a total demand of 638 [pax/h].

To alleviate in-vehicle crowding discomfort imposed on passengers when user cost is sensitive to on-board crowding levels, both vehicle size and service frequency are increased for both human-driven and automated vehicle fleet operations (see Fig. 1), i.e., the consideration of crowding discomfort externalities pushes solutions towards having larger and more frequent bus services. For instance, the results for Regensburg [see Fig. 1 (a)] show that vehicle sizes are increased at a similar rate in both human-driven and automated bus services, going from 12-m long buses for scenarios in which user cost is insensitive to on-board crowding levels to 15-m long buses for those scenarios in which on-board crowding is considered as a source of travel disutility when assessing user costs. However, service frequency is increased at a higher rate for automated vehicle fleet operations in the presence of on-board crowding effects. For example, service frequency increases by roughly 24%, going from 17 [veh/h] in the scenario of AV, ST, WOC to 21 [veh/h] in the scenario of AV, ST, WC, whereas it increases by 9%, going from 11 [veh/h] in the scenario of HV, ST, WOC to 12 [veh/h] in the scenario of HV, ST, WC. This result can be attributed to the fact that fleets of automated vehicles can reap much broader driving cost savings, thus opening up an opportunity for bus agencies to provide more frequent bus services with lower operating costs in spite of the increase of capital costs due to the larger fleet size requirement, i.e., the higher capital costs are compensated by a marked reduction in operating costs at higher frequencies and allow the deployment of larger fleets (Hatzenbühler et al., 2020; Tirachini and

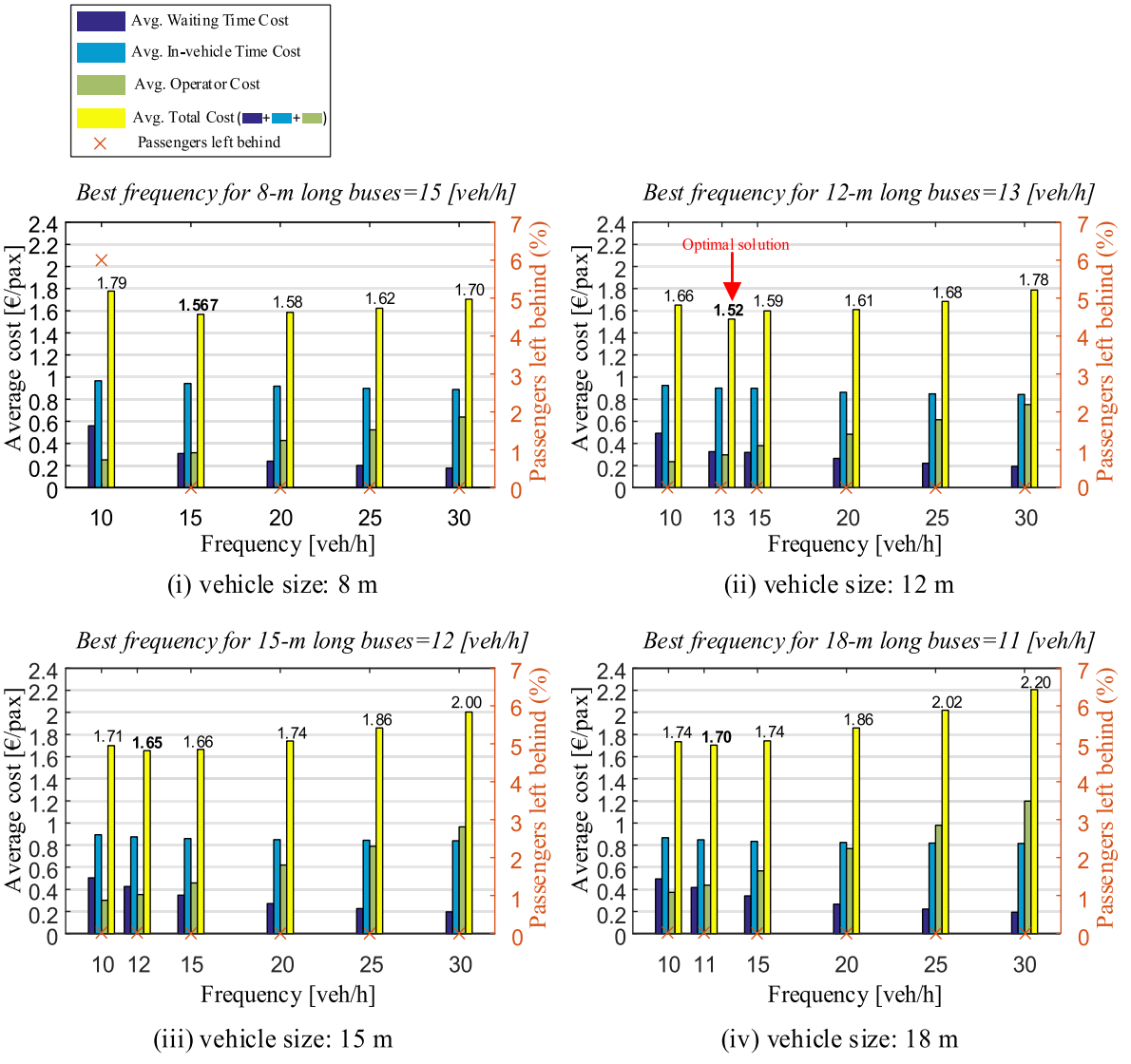

(a) AV, DT, WOC

Fig. 2. Comparison of cost elements for all scenarios with changes in frequencies and vehicle sizes (optimal vs. non-optimal deployment solutions), Regensburg case study.

Antoniou, 2020). Hence, vehicles can be operated with a higher optimal frequency to mitigate the user costs of crowding through the reduction of occupancy levels inside vehicles. As Fig. 1 (b) shows, the results have also the same pattern in the case of Santiago, however, vehicle sizes are increased from 12-m to 18-m long buses in the case of considering crowding as a source of dissatisfaction for users. This is because the given bus route in Santiago is known as an overcrowded corridor (5764 [pax/h]), in which vehicles operate at larger occupancy levels than Regensburg.

Overall, the deployment of automated bus services can significantly reduce occupancy levels inside vehicles, and thus in-vehicle crowding costs for on-board passengers, due to offering more frequent bus services with lower operating costs. In the case of Regensburg, assuming deterministic travel times, average occupancy goes down from 0.89 to 0.66 due to including crowding discomfort in the cost function for the case of human-driven vehicles, while the same figures are 0.62 and 0.39 for the case of automated vehicles, respectively. Therefore, the inclusion of crowding externalities in the model reduces average occupancy rates by 26% in the case of human-driven vehicles and 37% in the case of automated vehicles, a result that reinforces the relevance of automated vehicles in providing a higher standard of service for users under optimal operation conditions.

The assumption of stochastic travel times in dispatching scenarios (with the same standard deviation for human-driven and

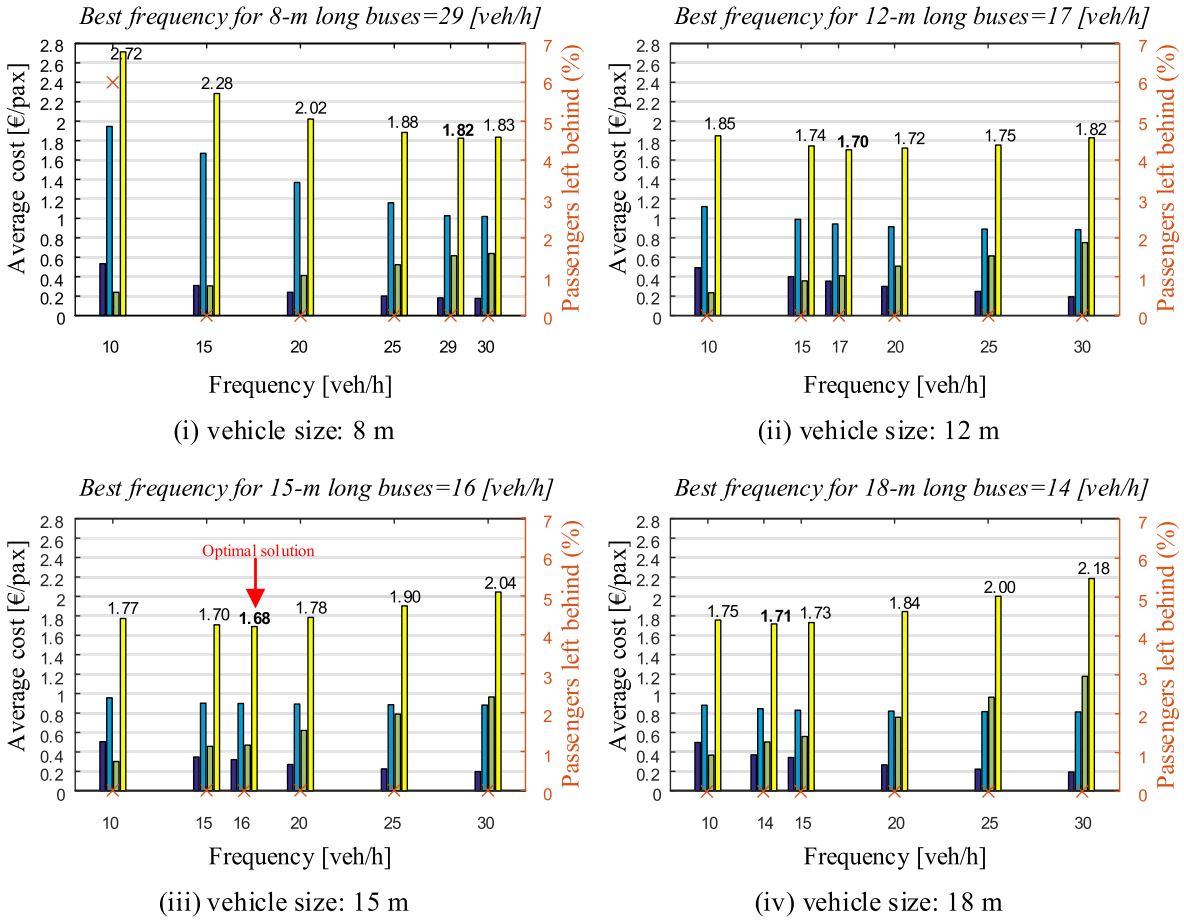

(b) AV, DT, WC

Fig. 2. (*continued*).

automated buses assumed in the base case) increases the optimal frequencies for both fleets of human-driven and automated buses, while vehicle sizes remain unchanged (e.g., see the scenarios of AV, DT, WOC and AV, ST, WOC in Fig. 1). Indeed, travel time stochasticity can lead to a further spread of irregularity among headways, thereby increasing passenger waiting times and reducing the reliability of a public transport system (Osuna and Newell, 1972). Hence, the setting of a higher service frequency can cope with the growth of passenger waiting times caused by travel time variability. As can be seen in Fig. 1 (a), the service frequency is increased at a higher rate for automated vehicle fleet operations, hovering around 30%, when travel times are assumed to be stochastic. This is because by deploying driverless vehicles, public transport operators can optimally provide more frequent services with lower operating costs to compensate for the growth of waiting times caused by travel time volatility in the scenarios with stochastic travel times. For example, service frequency is increased from a value of 16 [veh/h] in the scenario of AV, DT, WC to a value of 21 [veh/h] in the scenario of AV, ST, WC, whereas it is increased by 20%, going from 10 [veh/h] in the scenario of HV, DT, WC to 12 [veh/h] in the scenario of HV, ST, WC.

To better understand the trade-offs established between the user and operator costs during the process of finding the optimal solution (optimal service frequency and vehicle size) for both fleets of human-driven and automated vehicles, we provide information on the average costs at different levels of frequency and bus sizes for any given scenario in the case of Regensburg (see Fig. 2, and Fig. C1 presented in Appendix C). Indeed, in all scenarios, optimal and non-optimal deployment solutions can be easily compared to each other in terms of user and operator cost components, and therefore the total (social) costs. Overall, automated bus deployment scenarios lead to a lower social cost while operating at a higher optimal frequency.

4.4. The effects of automation on denied boarding

In this part, we examine the effects of automation on eliminating or reducing denied boardings. Given the high value of extra waiting time savings (Cats and Jenelius, 2018), the social costs of a public transportation service can climb dramatically if this problem

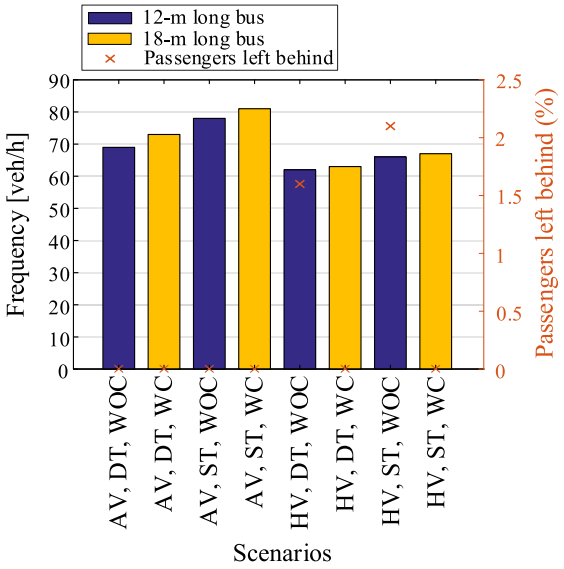

Fig. 3. Denied boardings in different scenarios, Santiago case study.

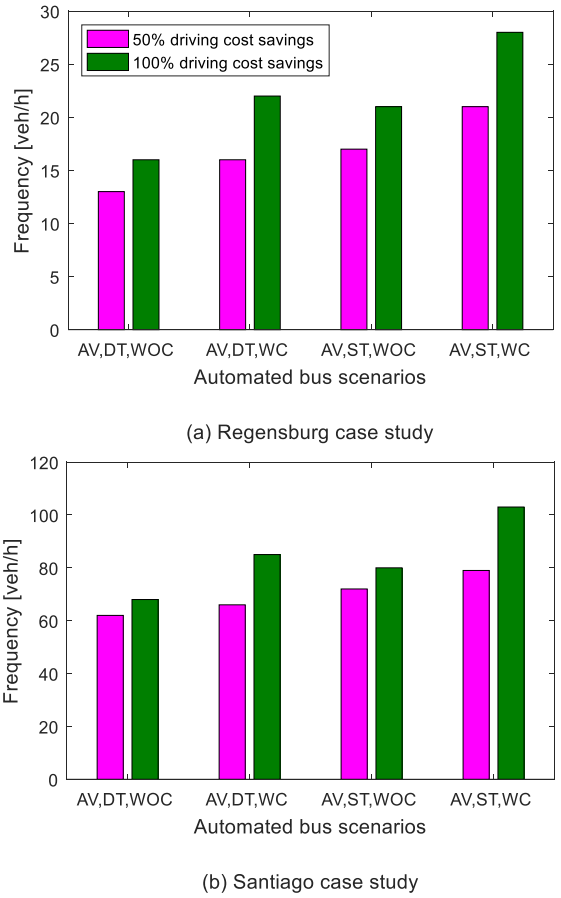

Fig. 4. Sensitivity to human driving cost savings due to automation.

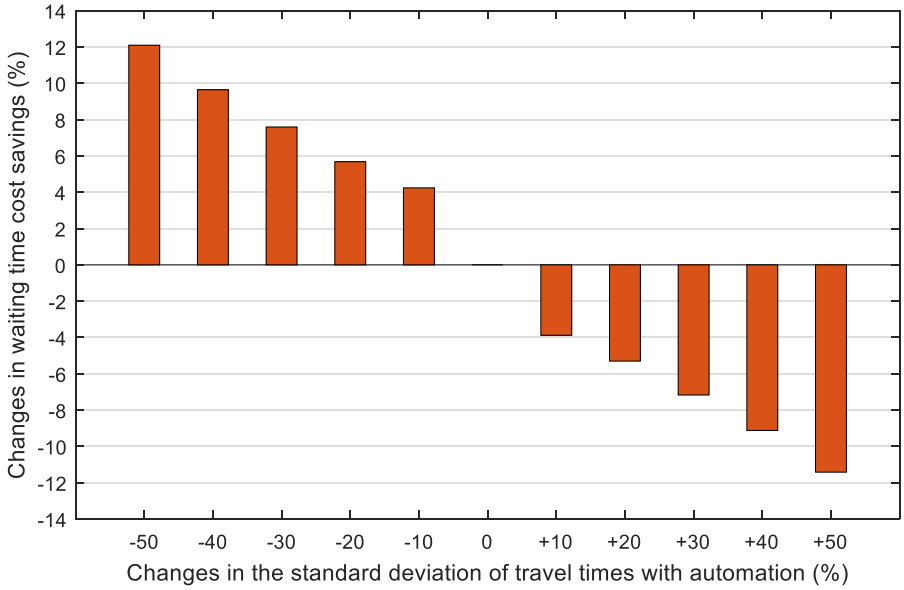

Fig. 5. Sensitivity to travel time variability due to automation.

is not effectively addressed, particularly on crowded bus corridors, such as the illustrative example of Santiago in our study.

For the case of Santiago, Fig. 3 shows the shares of passengers being left behind under the optimal solutions (optimal frequency and bus size). Buses are dispatched frequently enough under the optimal solutions, so that travelers are able to board the first arriving service. Nevertheless, the percentage of passengers failing to board is not zero in deployment scenarios of HV, DT, WOC (1.6% of denied boardings) and HV, ST, WOC (2.1% of denied boardings), both of which belong to human-driven vehicle fleet operations (HV), without consideration of crowding as increasing the value of travel time savings (WOC). In essence, in these two scenarios, the optimal frequency does not completely eliminate left-behind passengers, although the shares of passengers failing to board (1.6% and 2.1%) are relatively low. More precisely, in both scenarios, the user cost is insensitive to in-vehicle crowding levels, implying that the crowding cost component has no effect on pushing the optimal solution toward higher frequency levels in the favor of users. Besides, the human-driving cost plays a role against the increase of frequency. Overall, the high value of waiting time savings pushes the optimal deployment solutions toward the provision of sufficiently frequent services to properly meet passenger demand.

Enhancing service frequency is the most common way to mitigate rush-hour crowding effects (An et al., 2020). As indicated in Fig. 3, there are no passengers left behind in the operations of automated bus services, explained by the fact that automated vehicles can be optimally operated at higher frequencies with lower operating costs, thereby providing an unprecedented opportunity for public transport operators to efficiently counteract crowding-related problems in high-demand corridors, in which the multiple manifestations of crowding externalities (denied boarding, seat availability, on-board passenger discomfort) are more prominent.

4.5. Sensitivity to human driving cost savings due to automation

In the base case scenarios, we assumed 50% savings in human driving costs with automated vehicles. Now, we test cases in which human driving costs are fully (100%) saved with automation. As Fig. 4 shows, if automation capabilities can completely save human-related driven costs, automated bus scenarios are optimally pushed toward providing services with higher frequencies than the cases of 50% driving cost savings, and hence waiting and crowding costs are further reduced for users. Note that optimal vehicle sizes remain unchanged, which are similar to those obtained in the base case scenarios.

It is normally expected that, with full human driving cost savings, frequencies are increased at a higher degree for Regensburg than for Santiago, since the level of drivers' wages is larger in Germany than in Chile. Accordingly, when the user cost is insensitive to in-vehicle crowding levels, we see that frequencies are increased at a higher rate in the case of Regensburg (22%) than Santiago (12%). This is also in line with the findings of Tirachini and Antoniou (2020), who did not take crowding effects into account. However, in the presence of in-vehicle crowding effects, we interestingly see that there is not a salient difference between the increased rates, which are at 34% and 30% in Regensburg and Santiago respectively. This is because the crowding phenomenon is far more serious in the case of Santiago than Regensburg, which can persuade public transport providers (in light of full human driving cost savings) to boost optimal frequencies up to 30% in order to offset crowding discomfort costs exerted upon travelers in such a crowded bus corridor. Only a model, in which the value of travel time savings is sensitive to in-vehicle crowding levels, would be able to catch this effect. This result explicitly accentuates the importance of taking crowding discomfort externalities and their implications into account when assessing the actual benefits of automated public transport systems, especially for overcrowded bus corridors.

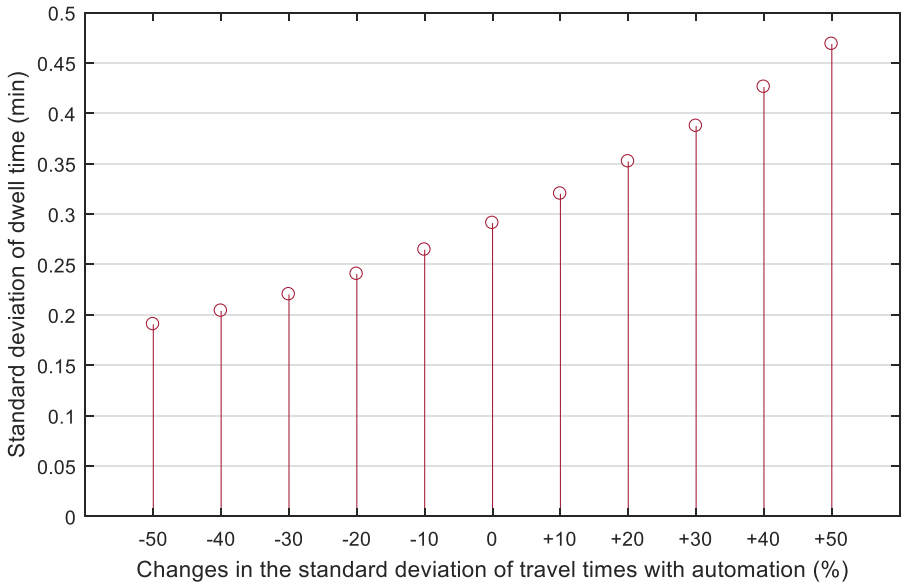

Fig. 6. Standard deviation of dwell times under different levels of change in travel time variability between stops with automation.

4.6. *Sensitivity to travel time uncertainty*

In the base case scenarios, we assumed that driving times between consecutive stops are stochastic (in ST scenarios), but at the same level of variability for both human-driven and automated bus services. In this part, we carry out a series of sensitivity analyses, in which travel time uncertainty is improved/degraded with automation through a reduction/rise in the standard deviation of travel times (values of σ_j in Eq. (16), used to model stochastic running times). We numerically investigate how an automated public transport system can yield larger/smaller savings in waiting time costs if the standard deviations of travel times are reduced/increased by $\pm$10, $\pm$20, $\pm$30, $\pm$40, and $\pm$50% due to automation (see Fig. 5).

As indicated in Fig. 5, our numerical results in Regensburg show that passenger waiting time costs could be saved by 12.1% if the technology of automation improved the reliability of public transport services through a reduction of travel time volatility by 50%. While waiting time is related to overall customer satisfaction (Tyrinopoulos and Antoniou, 2008; Dell'Olio et al., 2011), waiting time due to unreliability (e.g., travel time uncertainty) can have deeper negative consequences and be burdensome to public transport commuters (Rietveld et al., 2001; Van Lierop et al., 2018). The diversity in human driving habits can considerably aggravate travel time stochasticity in reality (Wang and Sun, 2020). Nonetheless, such differences in driving functions can be much less pronounced in the case of automated driving systems, due to the elimination of human interventions (Azad et al., 2019). Hence, public transport providers could potentially improve passengers' perceptions of reliability through the mitigation of unexpected waiting delays associated with unreliable services if automated public transport systems can offer a more reliable operation (more stable travel times) through leveraging full automation capabilities.

4.7. *Effects of automation and travel time stochasticity on dwell time regularity*

Dwell time variability can negatively affect bus operations and users' satisfaction, due to negative effects on the reliability of systems and predictability of trip times (Sun et al., 2014). Given the stochastic nature of public transport operations, the influences of driving time variations on the irregularity of dwell times at stations have been already investigated in the literature of travel time reliability for human-driven bus services (e.g., van Oort, 2014; van Oort, 2016; Schmidt et al., 2016). Overall, driving time volatility between stops can lead to a further spread of irregularity among vehicle dwell times due to poor service reliability, early or late services (van Oort, 2014). This is because travel time variations have adverse effects on load distributions, i.e., with a further growth of uncertainty in driving times between stops, passenger loads (the demand for getting on and off) will be irregularly distributed between buses on the same line, thus aggravating dwell time variability (Muñoz et al., 2020). An extra benefit of more regular operations is having more balanced passenger loads between vehicles.

To account for realistic operating conditions in the formulation of dwell time, we modeled flow-dependent dwell times which can vary at each station given alighting and boarding demands at that station. For example, a small delay due to driving time fluctuations provokes a rise in the number of travelers waiting at the next stop. This in turn leads to a rise in the dwell time, and consequently the bus delay and the risk of service unreliability are further exacerbated due to a positive feedback loop between the number of travelers waiting at stops, dwell times, and travel times between successive bus stops (Moreira-Matias et al., 2016).

Here, we numerically investigate how the deployment of an automated public transport system can lead to more regular/irregular dwell times at stops if the reliability of driving times between stops is improved/declined during operations with automation. To

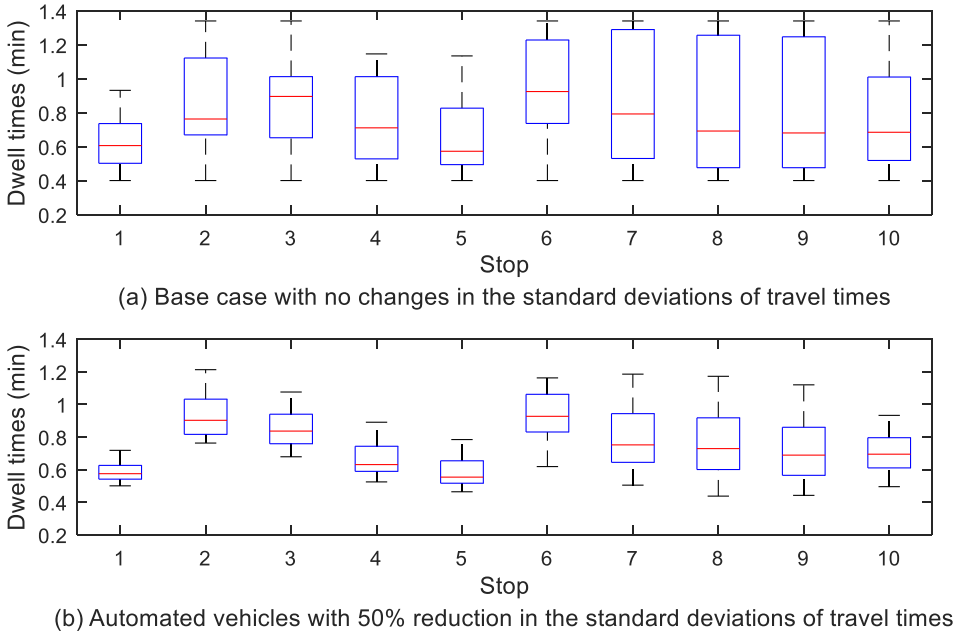

Fig. 7. Display of dispersion between dwell times of vehicles at each station.

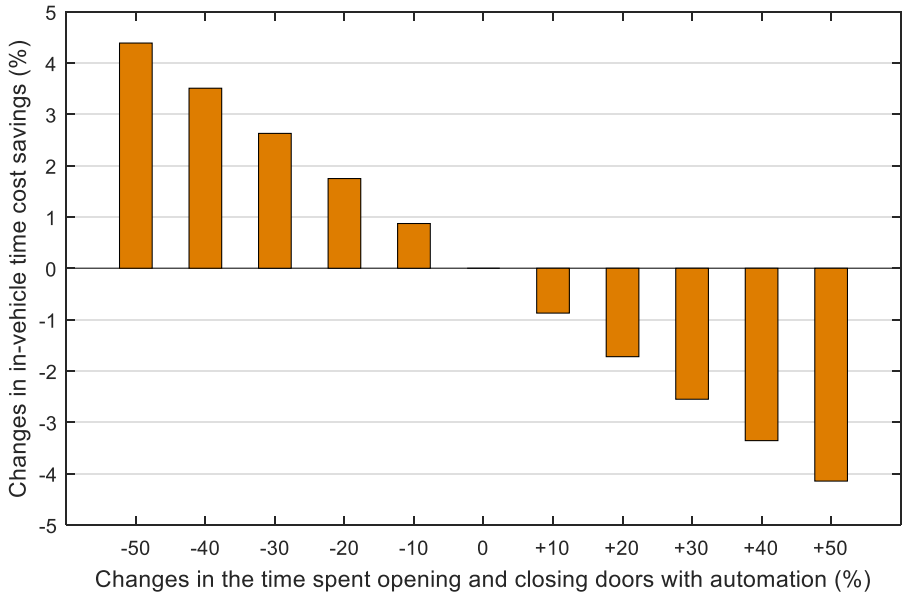

Fig. 8. Sensitivity to the time required for opening and closing doors with automation.

evaluate the dispersion in vehicles' dwell times affected by driving time variation levels, we measure the standard deviation of dwell times for automated vehicles, while changing the standard deviation of driving times between stops by ±10, ±20, ±30, ±40, and ±50%. Results are shown in Fig. 6 for the case of Regensburg at a given frequency of 20 [veh/h]. Note that the average length of dwell time is similarly 0.8 min in each case, as the total number of passengers alighting and boarding during the entire simulation time is the same for all the cases. As can be seen, the irregularity of dwell times is reduced if automated vehicles can provide a more stable operation with lower driving time variations. For instance, if the standard deviation of driving times between stops is reduced by 50% with automation, the standard deviation of dwell times at stops is decreased by 34%, dropping from 0.29 min to 0.19 min.

Besides, using a boxplot in Fig. 7, we illustrate the level of disparity in the dwell times of vehicles at each stop along the upstream direction. It is clearly observed that the dwell times of automated vehicles follow a more regular pattern with a reduction of 50% in travel time volatility compared to the base case (with no changes, 0%, in travel time variations).

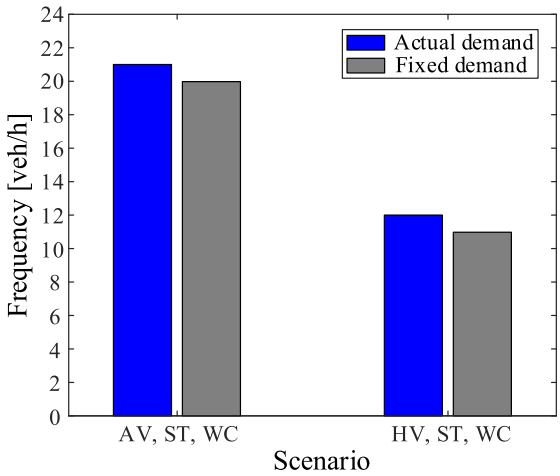

Fig. 9. Sensitivity to demand fluctuation.

4.8. Sensitivity to time spent opening and closing bus doors with automation

As described in Eq. (18), a part of the dwell time is related to the dead time needed for opening and closing bus doors, affecting bus stop delays. In the base case scenarios, we assumed that this time is the same for both human-driven and automated buses. Although this time might be larger or shorter with automation in reality, there appears to be no conclusive scientific evidence on this aspect yet.

On the one hand, this time might be increased with automation due to the inclusion of marginal safety factors when opening and closing doors without a human driver directly inspecting this procedure. Overall, the current programs of autonomous mobility services underline the need for operating automated vehicles with broader safety standards, due to security and safety reasons, i.e., given the operational obstacles and unknown aspects that might become apparent in practical terms, there is still a propensity toward the run of automated bus systems with a higher margin of safety in the current phase of deployment (Nemoto et al., 2020). Hence, due to the elimination of human checks formerly carried out by drivers inside human-driven buses, this dead time might be considered a bit longer for automated vehicles.

On the other hand, the technology of automation might be able to mitigate bus stop delays, associated with drivers' behavior and reaction times, through the elimination of human interventions. Moreover, for larger buses with more doors, drivers may need more time to check whether all doors are clear of passengers before activating the process of closing doors to leave stops (Tirachini et al., 2014). Automated vehicles, equipped with several advanced internal/external sensors and versatile monitoring technologies, can accurately detect the moment at which each door is clear of passengers. Hence, a shorter time might be needed for closing doors installed at different parts of a bus (e.g., front, middle, and back doors in a bus).

To assess the possible effects of vehicle automation on the process of opening and closing bus doors, we perform a series of sensitivity analysis tests, in which the relevant dead time is enlarged and reduced by ± 10, ± 20, ± 30, ± 40, and $\pm 50\%$ with automation (see Fig. 8). For instance, passengers' in-vehicle time costs are saved by 4.4% if such a time is reduced by 50% with automation.

4.9. Sensitivity to demand fluctuation

In this part, we aim to investigate the sensitivity of solutions to the demand fluctuation. Our base-case experiments were performed under 15-minute-dependent demand flows witnessing fluctuations during the simulation time (see Table A4 and Fig. A.1 in Appendix A). Now, we consider another demand case, under which passenger arrival rates remain fixed (without fluctuation) during the whole simulation period (7:00–9:00 AM), while the total demand is the same for both demand cases (see Table A5).

The optimal vehicle size and service frequency in the Regensburg case study are determined under this new case of passenger arrival rates. We see that the optimal vehicle size does not change. Nevertheless, as shown in Fig. 9, the optimal service frequency is reduced compared to the case of 15-minute-dependent arrival rates, tested in our base-case scenarios. For example, the optimal service frequency is reduced by about 8% and 5% in the deployment scenarios of HV, ST, WC and AV, ST, WC respectively. This is because although the total demand is the same for both actual (with fluctuation) and fixed (without fluctuation) demand cases, the passenger flow experiences a larger peak demand (i.e., peak inside the peak) in the actual demand case, observed around 7:45–8:00 AM (see Fig. A.1). Hence, the crowding-related problems (e.g., occupancy levels inside vehicles) can be increased at such maximum-load points, and therefore a higher level of frequency is optimally suggested to avoid the growth of crowding levels. Note that such effects are well captured in our crowding-sensitive model. This result accentuates the importance of considering demand volatility in the determination of service supply items, particularly at critical loading points (demand spikes) that can further exacerbate crowding-related issues.

Table 2
Crowding multipliers.

Load factor* F_{ij} (%)	α^{sit}	α^{stand}
0–75	0.86	—
75–100	0.95	—
100–125	1.05	1.62
125–150	1.16	1.79
150–175	1.27	1.99
175–200	1.40	2.20
200–	1.55	2.44

* Load factor inside a vehicle is defined as the ratio between the actual number of passengers inside the vehicle and the seating capacity of the vehicle [see Eq. (28)].
Source: Wardman and Whelan, 2011

Table 3
List of the simulated scenarios.

Scenarios	Vehicle technology		Travel time		In-vehicle crowding disutility effects	
	AV	**HV**	**DT**	**ST**	**WOC**	**WC**
AV, DT, WOC	✓		✓		✓	
AV, DT, WC	✓		✓			✓
AV, ST, WOC	✓			✓	✓	
AV, ST, WC	✓			✓		✓
HV, DT, WOC		✓	✓		✓	
HV, DT, WC		✓	✓			✓
HV, ST, WOC		✓		✓	✓	
HV, ST, WC		✓		✓		✓

AV: Automated vehicles.
HV: Human-driven vehicles.
DT: Deterministic travel times.
ST: Stochastic travel times.
WOC: Without in-vehicle crowding effects.
WC: With in-vehicle crowding effects.

Table 4
Sensitivity to crowding multipliers.

Reduction in crowding multipliers (%)	Scenario	Frequency (veh/h)
0	AV, ST, WC	81
	HV, ST, WC	67
20	AV, ST, WC	79
	HV, ST, WC	64
40	AV, ST, WC	77
	HV, ST, WC	61
60	AV, ST, WC	75
	HV, ST, WC	58

4.10. Sensitivity to crowding multipliers

We assess the sensitivity of solutions to changes in crowding cost parameters. In particular, lower levels of crowding multipliers have been reported in studies using revealed preference data in this context (Yap et al., 2020). Thus, we evaluate cases in which crowding multipliers (associated with load factors > 100% in Table 2) are reduced by 20%, 40%, and 60%. It should be noted that to avoid reaching multipliers that are smaller than 1, for an old multiplier α, the reduction is applied on (α-1), then it is summed by 1 to introduce the new multiplier. For example, for an old multiplier of 2.10 in the case of 50% reduction, the new multiplier would be 1.55.

In Table 4, the results are given for the main scenarios (HV, ST, WC vs. AV, ST, WC) in the case of Santiago. Overall, automated bus solutions witness a slower reduction in frequencies as crowding multipliers are reduced. For example, with a reduction of 60% in crowding multipliers, frequencies reduce by 7% (from 81 to 75[veh/h]) in the AV, ST, WC scenario, while they reduce by 13% (from 67 to 58 [veh/h]) in the HV, ST, WC scenario. In essence, since operating costs are more noticeable in human-driven bus operations, frequencies decline at a faster trend (in the favor of operators) when travelers are less sensitive to the crowding disutility. It should be noted that the optimal vehicle size is obtained as 18-m long buses in all cases.

Table 5
Sensitivity to the extra waiting time value.

Reduction in extra waiting time value (%)	Scenario	Frequency (veh/h)	Left-behind travelers (%)
0	AV, ST, WC	81	0
	HV, ST, WC	67	0
20	AV, ST, WC	81	0
	HV, ST, WC	67	0
40	AV, ST, WC	81	0
	HV, ST, WC	65	0.1
60	AV, ST, WC	81	0
	HV, ST, WC	61	2.1

Table 6
Sensitivity to user- and operator-oriented designs.

Cost multipliers	UCS with automation (%)	OCS with automation (%)
$\eta = 1.0, \mathscr{l} = 1.0$	19.8	15.8
$\eta = 1.2, \mathscr{l} = 1.0$	20.3	15.1
$\eta = 1.0, \mathscr{l} = 1.2$	19.1	16.4

UCS stands for user cost savings.
OCS stands for operator cost savings.

4.11. Sensitivity to extra waiting time values

In this part, we investigate the sensitivity of solutions to the value of extra waiting time savings caused by denied boarding. Particularly, compared to the value suggested by Cats et al. (2016) (as 3.5 times higher than the initial waiting time), lower values have been reported by recent studies employing revealed preference data in this context (Yap and Cats, 2021). Hence, we consider cases in which the value of extra waiting time savings is reduced by 20%, 40%, and 60%.

As shown in Table 5 for the case of Santiago, frequency solutions and the share of left-behind travelers are reported for the scenarios of HV, ST, WC and AV, ST, WC. Overall, vehicle automation still leads to the elimination of denied boardings. In essence, in such scenarios, to compensate for crowding discomfort and initial waiting time that has a high value of time savings, operating cost savings allow automated bus scenarios to still suggest high levels of frequency in the favor of users, and therefore optimal operations will not even become close to the critical denied boarding situations. Therefore, automated bus fleets can avoid denied boardings with higher degrees of robustness than human-driven fleets. Besides, our results show that the individual consideration of crowding discomfort in the planning of automated bus systems can even play a preventive role against denied boardings.

4.12. Sensitivity to user- and operator-oriented designs

In this part, we investigate the sensitivity of results to user- and operator-oriented design cases. For this purpose, we define two multipliers, as η and $\mathscr{l}$, to increase the value of user and operator cost savings respectively (i.e., the total cost in the objective function (1) can be expressed as $Z = \eta Z_p + \mathscr{l} Z_o$, considering the fact that such multipliers were considered as 1 in the base-case experiments). For example, $\eta = 1.2$ and $\mathscr{l} = 1.0$ imply that the current time valuations are increased by 20% for users, while the value of operator cost savings will remain unchanged the same as base-case valuations.

We test two scenarios: (i) $\eta = 1.2$ and $\mathscr{l} = 1.0$, and (ii) $\eta = 1.0$ and $\mathscr{l} = 1.2$ to represent user- and operator-oriented design cases respectively. Obviously, in line with the preference of users and operators, service frequency will increase and decrease in user- and operator-oriented design solutions respectively. However, cost savings achieved by vehicle automation deserve further analysis in such design conditions. Hence, comparing automated and human-driven bus scenarios, average cost savings with automation are reported for the case of Regensburg in Table 6. Overall, the results show that the savings of total costs with automation are roughly similar in both design cases, however, the benefits of automation are slightly more pronounced in the operator-oriented design case..

5. Concluding remarks

The present research develops a mathematical modeling framework to optimize service frequency and vehicle size for automated bus services, with stochastic travel times, time-dependent demand volumes, crowding externalities for both sitting and standing passengers, and the possibility of denied boarding due to capacity constraints. The model is able to estimate in-vehicle crowding discomfort at a microscopic level, bus by bus. Taking both passengers' and operators' costs into account, the objective of the model is to find the optimal service frequency and vehicle size with minimal total costs of a public transport service. Extensive experiments are performed under different scenarios to achieve a detailed assessment of the service and cost implications of the deployment of automated bus systems.

To evaluate the applicability of the proposed model, several deployment scenarios are simulated through the combination of different cases: (i) vehicle technology (human-driven or automated vehicles), (ii) travel time between stops (deterministic or stochastic

travel times), and (iii) crowding discomfort externalities (considering or ignoring in-vehicle crowding costs). Our experiments are executed for two real-world case studies in Regensburg, Germany, and Santiago, Chile. Besides, to further assess the possible effects of automation on the social costs of a public transportation service, an extensive range of sensitivity analysis tests are carried out on human driving cost savings with automation, travel time uncertainty, dwell time regularity, the time lost to open and close doors with automation, crowding multipliers, denied boarding saving values, and user- and operator-oriented design solutions.

The main findings of the present work are summarized as follows. When crowding matters to users, vehicle size and service frequency are increased for both human-driven and automated vehicle fleet operations. More precisely, vehicle size is increased at a similar rate for both human-driven and automated bus services, whereas service frequency is increased at a higher rate for fleets of automated vehicles. Therefore, under optimal levels of supply, automated vehicles can be run with lower occupancy levels than human-driven vehicles, increasing quality of service. This result is accruable if the deployment of automated vehicles can significantly save human-related driving costs, thus opening up an opportunity for public transport operators to provide more frequent bus services with lower operating costs. The deployment of automated bus services can significantly alleviate crowding-related capacity shortages as well, through a reduction or elimination of denied boarding problems. Therefore, our results explicitly accentuate the importance of taking crowding discomfort externalities into account when appraising the benefits of automated public transport systems, particularly for overcrowded bus corridors with a high volume of passengers during peak hours. Indeed, the actual benefits of automation might be underestimated if the detrimental effects of crowding on public transport users are not considered in the design and deployment of an automated bus system.

Second, the consideration of stochastic travel times between stops in the deployment scenarios results in optimal frequencies that are increased for both fleets of human-driven and automated driving buses; however, frequencies are increased at a higher rate for automated bus fleets. We numerically evaluate the possible effects of automation on travel time reliability through performing a number of sensitivity analysis tests on travel time variations. Results show that passenger waiting time costs will be reduced significantly if the technology of automation improves the reliability of public transport services through the reduction of travel time volatility.

Third, we numerically examine how the implementation of an automated public transport system can lead to more regular/irregular dwell times at stops if the reliability of driving times between stops is improved/declined during operations with automation. Results show that transit agencies will be efficiently able to suppress the stochastic nature of public transport operations in terms of travel time variability and dwell time irregularity if the deployment of future automated bus services can offer a more reliable operation with more predictable travel times, e.g., via leveraging full automation capabilities.

Finally, even though the potential of vehicle automation on reducing waiting times through increased frequencies is larger in high-income countries (Tirachini and Antoniou, 2020), we find that the final outcome is counterbalanced by the actual demand level in crowding-sensitive environments. In our case, the relative increase in optimal frequency was roughly similar in the Santiago and Regensburg case studies with the adoption of automated vehicles, because even though there is a greater potential of cost reduction in Regensburg due to larger driver cost savings, passenger demand in the Santiago case study was significantly larger, and therefore the crowding discomfort effect on pushing optimal frequencies up was stronger in Santiago than in Regensburg. Only a model, in which the value of travel time savings is sensitive to passenger occupancy levels, would be able to catch this effect.

In future investigations, it might be possible to take further decision variables into account, e.g., to determine the optimal number of seats for different sizes of automated buses together with optimal internal layout and space allocated to sitting and standing. Future studies will be required to develop a network modeling framework for the optimal design and deployment of automated bus services onto multiple lines at a bus network considering crowding externalities.

It should be noted that although the full enumeration method was able to address our single-line problem within acceptable computing efforts, it cannot be indeed an efficient method for addressing such a combinatorial optimization problem at large-scale network levels. Hence, future studies need to develop more efficient solution algorithms (such as branch and bound and *meta*-heuristic algorithms) to deal with the computational complexity of network-level instances. In future studies, the design of a simpler model including a smaller/minimum number of parameters would allow for a more efficient handling of parameters, avoiding the growth of errors in models with heavy computational burden, e.g., this aspect would be critical for future models intending to consider the possibility of operation with mixed fleets. A multi-period analysis with peak and off-peak periods is also an interesting direction for future research.

CRediT authorship contribution statement

Mohammad Sadrani: Conceptualization, Methodology, Formal analysis, Visualization, Software, Writing – review & editing. **Alejandro Tirachini:** Conceptualization, Methodology, Validation, Investigation, Writing – review & editing. **Constantinos Antoniou:** Conceptualization, Methodology, Validation, Investigation, Project administration, Writing – review & editing.

Declaration of Competing Interest

The authors declare that they have no known competing financial interests or personal relationships that could have appeared to influence the work reported in this paper.

Acknowledgments

This work was supported by the Bundesministerium für Bildung und Forschung (BMBF) funded cluster MCube (COLTOC project, Germany, funding number: 5320073), by the TUM International Graduate School of Science and Engineering-IGSSE (project 12.04-MO3, Germany), and by the European Union Horizon 2020 Research and Innovation Programme under grant agreement N.815069 (MOMENTUM project). Also, the second author is grateful for the support of ANID Chile (Grant PIA/BASAL AFB180003).

Appendix A. Input parameters for model application: Case studies in Germany and Chile

For stochastic running times, a lognormal distribution is considered with the mean of 2.2 and 3.5 min and the standard deviations of 0.6 and 0.8 min for Regensburg and Santiago respectively.

In the current programs of vehicle automation, the vast majority of studies in the literature have pointed out that automated buses might be operated at lower speeds than human-driven ones, owing to safety-related concerns considered more widely in the current phase of operation with automated vehicles in cities (e.g., Ainsalu et al., 2018; Pernestål et al., 2018; Kyriakidis et al., 2019; Zhang et al., 2019; Tirachini and Antoniou, 2020; Heikoop et al., 2020). Consistent with the available literature on automated buses, we also assume that automated bus systems are slower, operating with longer mean travel times by 10 percent.

Size-dependent parameters are presented in Tables A2 and A3, taken from the work of Tirachini and Antoniou (2020) for both Germany and Chile.

It should be noted that the bus capacity is commonly assumed to be larger in Santiago, due to a higher density of standees normally accepted among public transport users in Santiago compared to Germany (Tirachini and Antoniou, 2020).

In Table A4, time-dependent passenger arrival rates are listed for the bus corridor in Regensburg during a planning period extending from 7:00 to 9:00 AM. As can be seen, we provide a 15-minute-dependent passenger demand (remaining fixed during each interval of 15 min). Moreover, in Table A5, we provide a fixed demand case used for performing a sensitivity analysis test in subsection 4.9. The values in Table A5 are derived from averaging arrival flow rates within the corresponding 15-minute intervals, given in Table A4.

Table A1
Parameter values for model application.

Parameter	Unit	Regensburg	Santiago
Total demand	pax/h	638	5764
Route length	km	6.3	9
Minimum frequency	veh/h	5	15
Maximum frequency	veh/h	40	120
Acceleration time	s	6	6
Deceleration time	s	6	6
Time for opening and closing bus doors	s	6	6
Average alighting time per passenger	s/pax	1.5	1.5
Average boarding time per passenger	s/pax	2.5	2.5
Monetary value of in-vehicle time*	€/h	5.2	2.9
Monetary value of initial waiting time*	€/h	11.4	3.5
Monetary value of extra waiting time due to denied boarding**	€/h	39.9	12.3
Driver cost*	€/veh-h	15.3	6.2
Reduced human driving cost automation (base case scenarios)	%	50	50
Reduced running cost automation	%	10	10

* Source: Tirachini and Antoniou (2020).
** The monetary value of extra waiting time due to denied boarding is 3.5 times higher than that of initial waiting time (Cats et al., 2016).

Table A2
Size-dependent parameters, Regensburg.

Parameter	Unit	Mini bus	Standard bus	Rigid bus	Articulated bus
Vehicle length	m	8	12	15	18
Vehicle capacity	pax/veh	44	70	90	110
No. of seats	–	25	40	50	60
No. of doors	–	1	2	3	4
PA = PB*	%	100	60	43	30
Vehicle running cost	€/veh-km	0.7	1.1	1.3	1.6
Vehicle capital cost	€/veh-h	7.7	11.5	14.7	17.2
Increased capital cost automation	%	37	25	25	24

* PA and PB are the proportions of passengers getting off and on through the busiest door respectively.
Source: Tirachini and Antoniou, 2020

Table A3
Size-dependent parameters, Santiago.

Parameter	Unit	Mini bus	Standard bus	Rigid bus	Articulated bus
Vehicle length	m	8	12	15	18
Vehicle capacity	pax/veh	50	90	115	145
No. of seats	–	25	40	50	60
No. of doors	–	1	2	3	4
PA = PB*	%	100	60	43	30
Vehicle running cost	€/veh-km	0.4	0.7	0.9	1.1
Vehicle capital cost	€/veh-h	5.2	7.7	9.5	11.6
Increased capital cost automation	%	37	25	25	24

Source: Tirachini and Antoniou, 2020

Table A4
15-minute-dependent passenger arrival rates (unit: pax/min).

Stop	7:00-7:15	7:15-7:30	7:30-7:45	7:45-8:00	8:00-8:15	8:15-8:30	8:30-8:45	8:45-9:00
1	0.80	0.86	0.95	1.16	1.10	1.00	0.95	0.85
2	0.25	0.27	0.27	0.33	0.29	0.27	0.25	0.23
3	0.20	0.21	0.21	0.26	0.25	0.23	0.21	0.20
4	0.32	0.34	0.34	0.36	0.35	0.30	0.27	0.25
5	0.26	0.28	0.31	0.38	0.36	0.35	0.29	0.27
6	0.50	0.52	0.65	0.75	0.60	0.71	0.65	0.61
7	0.21	0.23	0.24	0.30	0.26	0.25	0.22	0.20
8	0.86	0.91	0.79	0.93	0.95	0.81	0.77	0.71
9	0.46	0.49	0.56	0.68	0.65	0.62	0.55	0.51
10	0.64	0.69	0.7	0.83	0.82	0.78	0.71	0.66
11	0.23	0.25	0.27	0.30	0.29	0.27	0.23	0.21
12	0.00	0.00	0.00	0.00	0.00	0.00	0.00	0.00
13	0.81	0.76	1.00	1.15	1.10	0.95	1.00	0.95
14	0.33	0.35	0.34	0.28	0.37	0.20	0.19	0.18
15	0.14	0.14	0.21	0.26	0.22	0.30	0.14	0.13
16	0.42	0.44	0.39	0.45	0.26	0.28	0.29	0.28
17	0.31	0.33	0.30	0.44	0.36	0.33	0.38	0.35
18	0.45	0.47	0.76	0.64	0.63	0.78	0.58	0.54
19	0.25	0.26	0.24	0.19	0.20	0.21	0.25	0.23
20	0.91	0.95	0.74	0.88	0.76	0.49	0.53	0.65
21	0.56	0.59	0.67	0.88	0.59	0.78	0.50	0.46
22	0.71	0.74	0.83	0.83	0.54	0.50	0.77	0.72
23	0.27	0.28	0.34	0.18	0.35	0.23	0.18	0.21
24	0.00	0.00	0.00	0.00	0.00	0.00	0.00	0.00

Table A5
Fixed passenger arrival rates (unit: pax/min).

Stop	7:00–9:00
1	0.96
2	0.27
3	0.22
4	0.32
5	0.31
6	0.62
7	0.24
8	0.84
9	0.57
10	0.73
11	0.26
12	0
13	0.95
14	0.28
15	0.19
16	0.35
17	0.35
18	0.61
19	0.23
20	0.74
21	0.63
22	0.71
23	0.26
24	0

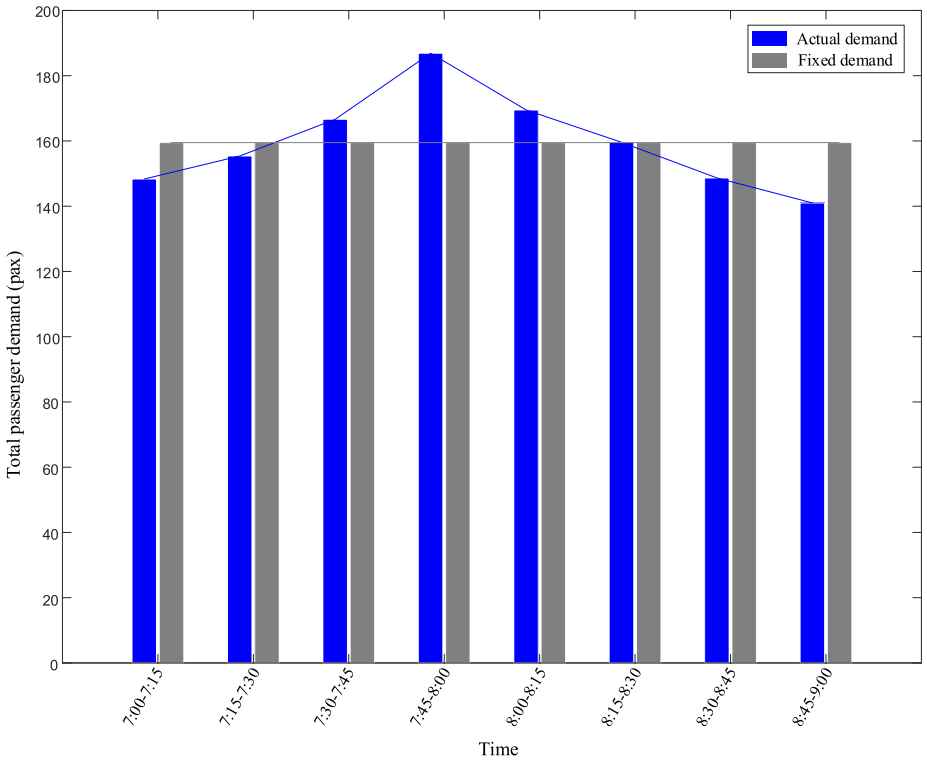

Fig. A1. Total passenger demand entering the bus route during each interval of 15 min, as listed in Tables A4 and A5.

Appendix B. Solution procedure

The main steps of the solution procedure are described here, including the full enumeration (FE) and the Monte Carlo Simulation (MCS) algorithms.

Algorithm 1. (*The main steps of the full enumeration method*)

- **Step (1):** Set the candidate values for vehicle size and frequency (as decision variables), which are respectively confined to the given discrete sets of {8,12,15,18} [meters] and $\{f_{\min}, f_{\min}+1, \cdots, f_{\max}-1, f_{\max}\}$ [veh/h] in the proposed problem.
- **Step (2):** In each deployment scenario, while vehicle size is fixed (for any given size) during the simulation time, set parameters **&** enumerate over all the frequency values to evaluate all the possible combinations of vehicle size and frequency (for a better view of this step, see Fig. 2 or Fig. C.1), i.e., step (2) includes (2.1) **&** (2.2):
  (2.1). Set input parameters. Note that the size-dependent parameters are set based on the vehicle size fixed.
  (2.2). Evaluate the objective function value [in Eq. (1)] for each combination of vehicle size and frequency using Algorithm 2. In essence, to handle the uncertainty of stochastic travel times, each possible solution is evaluated over several replications through the MCS method (see Algorithm 2 for more details).
- **Step (3):** Return the best-found solution (among all the combinations of vehicle size and frequency) leading to the minimum total cost value.

Algorithm 2. (*The main steps of the Monte Carlo Simulation method*)

(i) **Set the MCS parameters:** Set the counter of simulations m and its initial value as 1; let $\overline{Z}^{(m)}$ denote the estimated objective function value in Eq. (1); set the maximum number of simulations as $M_{max} = 1000$.

(ii) **Perform travel time sampling:** The bus travel time between each two consecutive stops is a random variable with predetermined mean and standard deviation values. For each bus service, sample the travel time between stops $j-1$ and j (i.e., T^{r}_{ij}) through Eq. (16) based on its log-normal distribution, where $i = 1, 2, \cdots, N_v$ and $j = 2, 3, \cdots, N_s$.

(iii) **Compute the variables:** Based on the sampled travel time value, update the relevant variables in the solution using Eqs. (13)–(32), including bus motion and passenger flow calculations: bus travel time, headways, dwell time, arrival/departure time at each stop, the number of passengers waiting, alighting and successfully boarding the vehicle, failing to board, sitting and standing inside the vehicle.

(iv) **Compute the objective function value:** Based on Eq. (1), compute and update the objective value $Z^{(m)}$, and the final output of objective value is determined through the average value of simulation samples:

$$\overline{Z}^{(m)} = \frac{Z^{(m)} + (m-1).\overline{Z}^{(m-1)}}{m} \quad (33)$$

(v) **Check the stopping condition:** Increase the number of simulations by 1, i.e., $m = m + 1$. If $m < M_{max}$, return to step (ii); otherwise, stop and output the estimated objective function value $\overline{Z} = \overline{Z}^{(m)}$.

Appendix C. Trade-offs between user and operator costs in scenarios c-h

See Fig. C1.

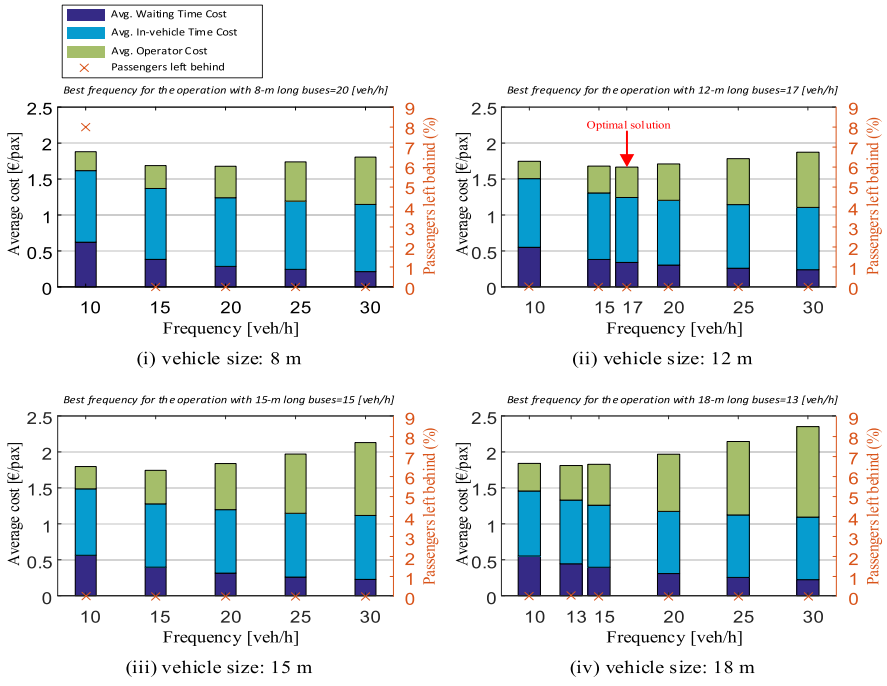

(c) AV,ST,WOC

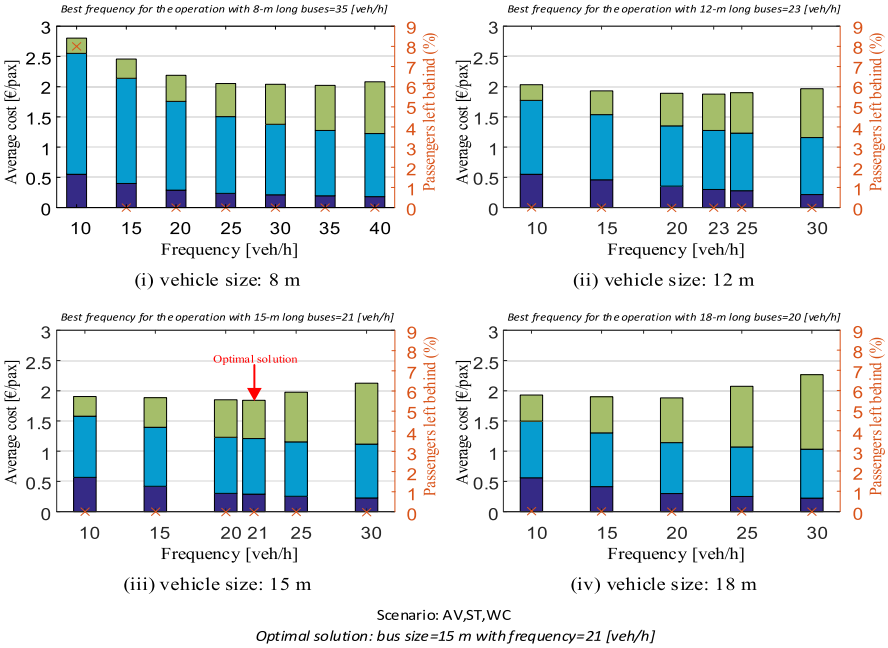

(d) AV,ST,WC

Fig. C1. Comparison of cost elements for all scenarios with changes in frequencies and vehicle sizes (optimal vs. non-optimal deployment solutions), Regensburg case study.

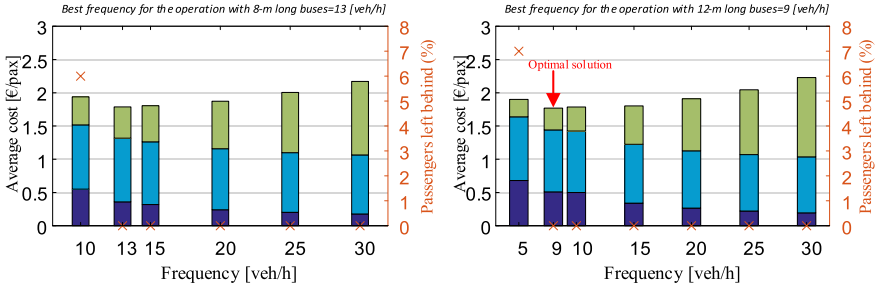

(i) vehicle size: 8 m

(ii) vehicle size: 12 m

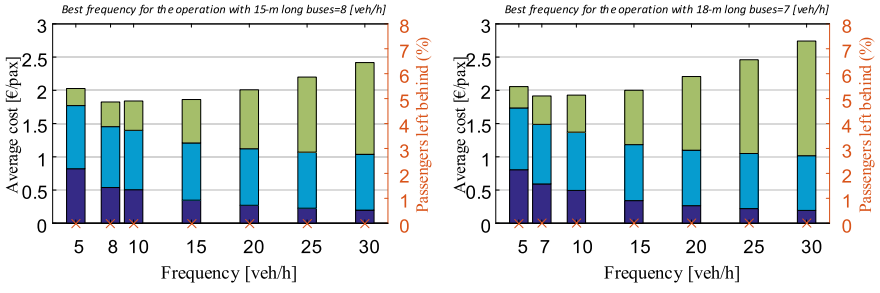

(iii) vehicle size: 15 m

(iv) vehicle size: 18 m

Scenario: HV,DT,WOC

Optimal solution: bus size=12 m with frequency=9 [veh/h]

(e) HV,DT,WOC

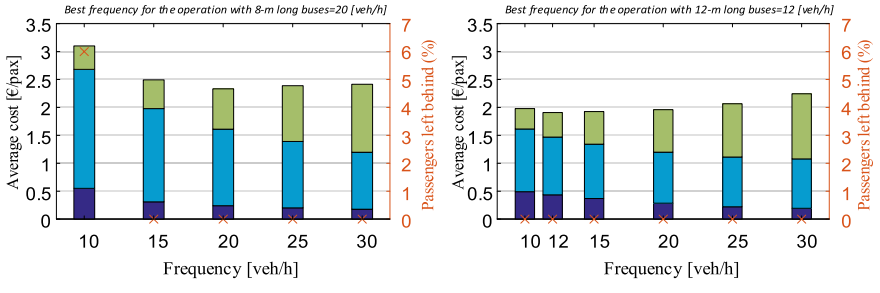

(i) vehicle size: 8 m

(ii) vehicle size: 12 m

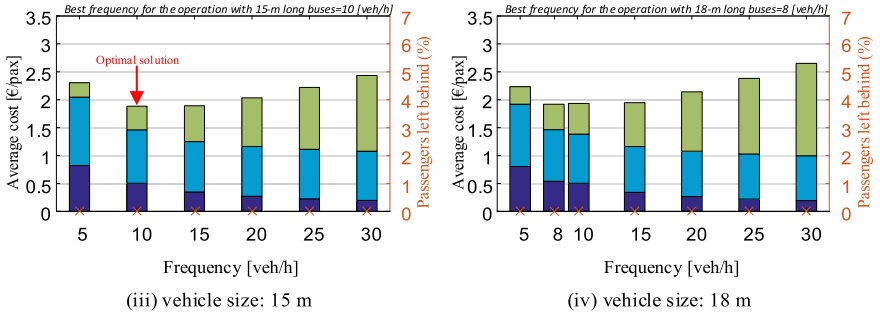

(iii) vehicle size: 15 m

(iv) vehicle size: 18 m

Scenario: HV,DT,WC

Optimal solution: bus size=15 m with frequency=10 [veh/h]

(f) HV,DT,WC

Fig. C1. (*continued*).

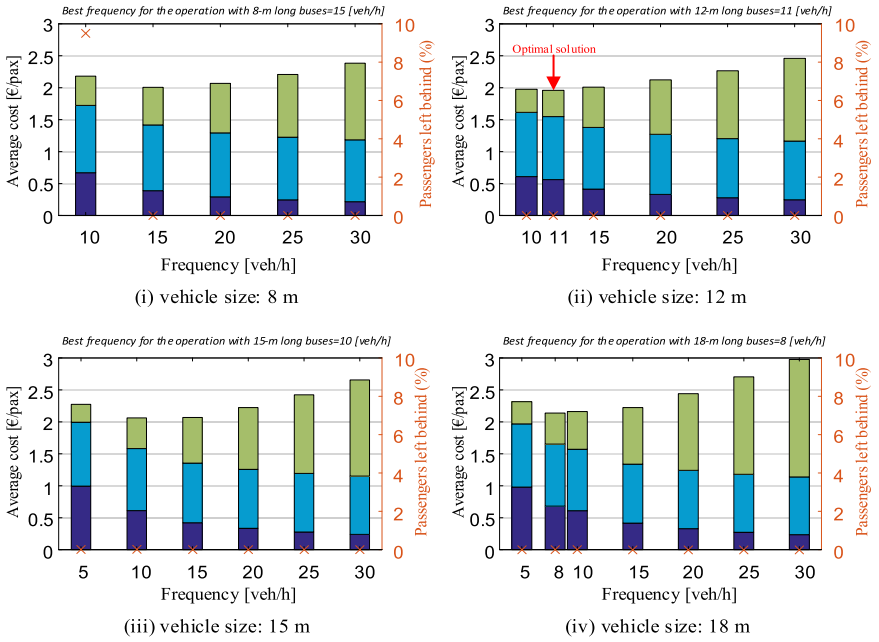

(i) vehicle size: 8 m (ii) vehicle size: 12 m

(iii) vehicle size: 15 m (iv) vehicle size: 18 m

Scenario: HV,ST,WOC

Optimal solution: bus size=12 m with frequency=11 [veh/h]

(g) HV,ST,WOC

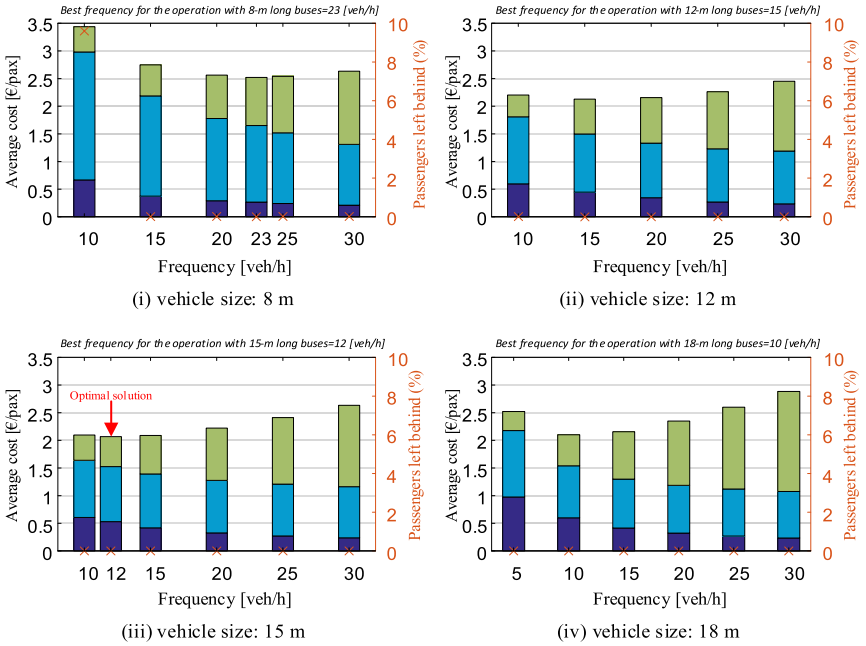

(i) vehicle size: 8 m (ii) vehicle size: 12 m

(iii) vehicle size: 15 m (iv) vehicle size: 18 m

Scenario: HV,ST,WC

Optimal solution: bus size=15 m with frequency=12 [veh/h]

(h) HV,ST,WC

Fig. C1. (*continued*).

References

Abe, R., 2019. Introducing autonomous buses and taxis: Quantifying the potential benefits in Japanese transportation systems. Transp. Res. Part A Policy Pract. 126, 94–113.

Agrawal, K., Suman, H.K., Bolia, N.B., 2020. Frequency optimization models for reducing overcrowding discomfort. Transp. Res. Rec. 2674, 160–171.

Ainsalu, J., Arffman, V., Bellone, M., Ellner, M., Haapamäki, T., Haavisto, N., Josefson, E., Ismailogullari, A., Lee, B., Madland, O., 2018. State of the art of automated buses. Sustainability 10, 3118.

Alessandrini, A., Holguin, C., Parent, M., 2011. Advanced transport systems showcased in La Rochelle. In: in: 2011 14th International IEEE Conference on Intelligent Transportation Systems (ITSC). IEEE, pp. 896–900.

An, Q., Fu, X., Huang, D., Cheng, Q., Liu, Z., 2020. Analysis of adding-runs strategy for peak-hour regular bus services. Transp. Res. Part E Logist. Transp. Rev. 143, 102100.

Azad, M., Hoseinzadeh, N., Brakewood, C., Cherry, C.R., Han, L.D., 2019. Fully autonomous buses: A literature review and future research directions. J. Adv, Transp, p. 2019.

Badia, H., Jenelius, E., 2021. Design and operation of feeder systems in the era of automated and electric buses. Transp. Res. Part A Policy Pract. 152, 146–172.

Bansal, P., Kockelman, K.M., 2017. Forecasting Americans' long-term adoption of connected and autonomous vehicle technologies. Transp. Res. Part A Policy Pract. 95, 49–63.

Bartholdi III, J.J., Eisenstein, D.D., 2012. A self-coördinating bus route to resist bus bunching. Transp. Res. Part B Methodol. 46, 481–491.

Batarce, M., Muñoz, J.C., de Dios Ortúzar, J., 2016. Valuing crowding in public transport: Implications for cost-benefit analysis. Transp. Res. Part A Policy Pract. 91, 358–378.

Bösch, P.M., Becker, F., Becker, H., Axhausen, K.W., 2018. Cost-based analysis of autonomous mobility services. Transp. Policy 64, 76–91.

Brinckerhoff, P., 2013. Group, K.; Texas, A.: Transit capacity and quality of service manual. Transit Cooperative Highway Research Program (TCRP) Report 165. Transp. Res. Board Washington, DC.

Cao, Z., Ceder, A.A., 2019. Autonomous shuttle bus service timetabling and vehicle scheduling using skip-stop tactic. Transp. Res. Part C Emerg. Technol. 102, 370–395.

Cao, Z., Ceder, A.A., Zhang, S., 2019. Real-time schedule adjustments for autonomous public transport vehicles. Transp. Res. Part C Emerg. Technol. 109, 60–78.

Cats, O., Glück, S., 2019. Frequency and vehicle capacity determination using a dynamic transit assignment model. Transp. Res. Rec. 2673, 574–585.

Cats, O., Jenelius, E., 2018. Beyond a complete failure: the impact of partial capacity degradation on public transport network vulnerability. Transp. B Transp. Dyn. 6, 77–96.

Cats, O., Larijani, A.N., Koutsopoulos, H.N., Burghout, W., 2011. Impacts of Holding Control Strategies on Transit Performance: Bus Simulation Model Analysis. Transp. Res. Rec. 2216, 51–58. https://doi.org/10.3141/2216-06.

Cats, O., West, J., Eliasson, J., 2016. A dynamic stochastic model for evaluating congestion and crowding effects in transit systems. Transp. Res. Part B Methodol. 89, 43–57. https://doi.org/10.1016/j.trb.2016.04.001.

Ceder, A.A., 2021. Syncing sustainable urban mobility with public transit policy trends based on global data analysis. Sci. Rep. 11, 1–13.

Chiraphadhanakul, V., Barnhart, C., 2013. Incremental bus service design: combining limited-stop and local bus services. Public Transp. 5, 53–78.

Cortés, C.E., Jara-Díaz, S., Tirachini, A., 2011. Integrating short turning and deadheading in the optimization of transit services. Transp. Res. Part A Policy Pract. 45, 419–434.

Dai, Z., Liu, X.C., Chen, X., Ma, X., 2020. Joint optimization of scheduling and capacity for mixed traffic with autonomous and human-driven buses: A dynamic programming approach. Transp. Res. Part C Emerg. Technol. 114, 598–619.

Dai, Z., Ma, X., Chen, X., 2019. Bus travel time modelling using GPS probe and smart card data: a probabilistic approach considering link travel time and station dwell time. J. Intell. Transp. Syst. 23, 175–190.

De Palma, A., Kilani, M., Proost, S., 2015. Discomfort in mass transit and its implication for scheduling and pricing. Transp. Res. Part B Methodol. 71, 1–18.

Delgado, F., Munoz, J.C., Giesen, R., 2012. How much can holding and/or limiting boarding improve transit performance? Transp. Res. Part B Methodol. 46, 1202–1217. https://doi.org/10.1016/j.trb.2012.04.005.

Dell'Olio, L., Ibeas, A., Cecin, P., 2011. The quality of service desired by public transport users. Transp. Policy 18, 217–227.

Distler, V., Lallemand, C., Bellet, T., 2018. Acceptability and acceptance of autonomous mobility on demand: The impact of an immersive experience. In: Proceedings of the 2018 CHI Conference on Human Factors in Computing Systems, pp. 1–10.

Dong, X., DiScenna, M., Guerra, E., 2019. Transit user perceptions of driverless buses. Transportation (Amst). 46, 35–50.

Drabicki, A., Kucharski, R., Cats, O., Szarata, A., 2020. Modelling the effects of real-time crowding information in urban public transport systems. Transp. A Transp. Sci. 1–39.

Durán-Hormazábal, E., Tirachini, A., 2016. Estimation of travel time variability for cars, buses, metro and door-to-door public transport trips in Santiago. Chile. Res. Transp. Econ. 59, 26–39.

Eden, G., Nanchen, B., Ramseyer, R., Evéquoz, F., 2017. Expectation and experience: Passenger acceptance of autonomous public transportation vehicles. IFIP Conf. Hum.-Computer Interaction. Springer 360–363.

Fielbaum, A., 2019. Strategic public transport design using autonomous vehicles and other new technologies. Int. J. Intell. Transp. Syst. Res. 1–9.

Fu, L., Liu, Q., Calamai, P., 2003. Real-time optimization model for dynamic scheduling of transit operations. Transp. Res. Rec. 1857, 48–55.

Furth, P.G., Wilson, N.H.M., 1981. Setting frequencies on bus routes: theory and practice. Transp. Res. Rec. 818, 1–7.

Gao, Y., Kroon, L., Schmidt, M., Yang, L., 2016. Rescheduling a metro line in an over-crowded situation after disruptions. Transp. Res. Part B Methodol. 93, 425–449. https://doi.org/10.1016/j.trb.2016.08.011.

Gkiotsalitis, K., 2020. Stop-skipping in rolling horizons. Transp. A Transp. Sci. 1–29.

Gkiotsalitis, K., Cats, O., 2018. Reliable frequency determination: Incorporating information on service uncertainty when setting dispatching headways. Transp. Res. Part C Emerg. Technol. 88, 187–207.

Gkiotsalitis, K., Schmidt, M., van der Hurk, E., 2022. Subline frequency setting for autonomous minibusses under demand uncertainty. Transp. Res. Part C Emerg. Technol. 135, 103492.

Gkiotsalitis, K., Van Berkum, E.C., 2020a. An exact method for the bus dispatching problem in rolling horizons. Transp. Res. Part C Emerg. Technol. 110, 143–165.

Gkiotsalitis, K., Van Berkum, E.C., 2020b. An analytic solution for real-time bus holding subject to vehicle capacity limits. Transp. Res. Part C Emerg. Technol. 121, 102815.

Hamdouch, Y., Ho, H.W., Sumalee, A., Wang, G., 2011. Schedule-based transit assignment model with vehicle capacity and seat availability. Transp. Res. Part B Methodol. 45, 1805–1830.

Hatzenbühler, J., Cats, O., Jenelius, E., 2020. Transitioning towards the deployment of line-based autonomous buses: Consequences for service frequency and vehicle capacity. Transp. Res. Part A Policy Pract. 138, 491–507.

Heikoop, D.D., Velasco, J.P.N., Boersma, R., Bjørnskau, T., Hagenzieker, M.P., 2020. Automated bus systems in Europe: a systematic review of passenger experience and road user interaction.

Hickman, M.D., 2001. An analytic stochastic model for the transit vehicle holding problem. Transp. Sci. 35, 215–237.

Hörcher, D., De Borger, B., Seifu, W., Graham, D.J., 2020. Public transport provision under agglomeration economies. Reg. Sci. Urban Econ. 81, 103503.

Hörcher, D., Graham, D.J., 2018. Demand imbalances and multi-period public transport supply. Transp. Res. Part B Methodol. 108, 106–126.

Hörcher, D., Graham, D.J., Anderson, R.J., 2018. The economics of seat provision in public transport. Transp. Res. Part E Logist. Transp. Rev. 109, 277–292.

Hörcher, D., Graham, D.J., Anderson, R.J., 2017. Crowding cost estimation with large scale smart card and vehicle location data. Transp. Res. Part B Methodol. 95, 105–125.

Hörcher, D., Tirachini, A., 2021. A review of public transport economics. Econ. Transp. 25, 100196.

Jara-Díaz, S., Gschwender, A., 2003. Towards a general microeconomic model for the operation of public transport. Transp. Rev. 23, 453–469.
Jenelius, E., 2020. Personalized predictive public transport crowding information with automated data sources. Transp. Res. Part C Emerg. Technol. 117, 102647.
Jenelius, E., 2018. Public transport experienced service reliability: Integrating travel time and travel conditions. Transp. Res. Part A Policy Pract. 117, 275–291.
Jiang, X., Guo, X., Ran, B., 2014. 2014. Optimization model for headway of a suburban bus route. Math. Probl, Eng.
Klumpenhouwer, W., Wirasinghe, S.C., 2016. Cost-of-crowding model for light rail train and platform length. Public Transp. 8, 85–101.
Kyriakidis, M., de Winter, J.C.F., Stanton, N., Bellet, T., van Arem, B., Brookhuis, K., Martens, M.H., Bengler, K., Andersson, J., Merat, N., 2019. A human factors perspective on automated driving. Theor. Issues Ergon. Sci. 20, 223–249.
Lazarus, J., Shaheen, S., Young, S.E., Fagnant, D., Voege, T., Baumgardner, W., Fishelson, J., Lott, J.S., 2018. Shared automated mobility and public transport, in: Road Vehicle Automation 4. Springer, pp. 141–161.
Liu, Z., Yan, Y., Qu, X., Zhang, Y., 2013. Bus stop-skipping scheme with random travel time. Transp. Res. Part C Emerg. Technol. 35, 46–56.
Lu, H., Burge, P., Heywood, C., Sheldon, R., Lee, P., Barber, K., Phillips, A., 2018. The impact of real-time information on passengers' value of bus waiting time. Transp. Res. Procedia 31, 18–34.
Lutin, J.M., 2018. Not If, but when: autonomous driving and the future of transit. J. Public Transp. 21, 10.
Moreira-Matias, L., Cats, O., Gama, J., Mendes-Moreira, J., De Sousa, J.F., 2016. An online learning approach to eliminate Bus Bunching in real-time. Appl. Soft Comput. 47, 460–482.
Mosquet, X., Dauner, T., Lang, N., Russmann, M., Mei-Pochtler, A., Agrawal, R., Schmieg, F., 2015. Revolution in the Driver's seat: the road to autonomous vehicles. Bcg. perspectives, Boston Consulting Group, April 21, 2015.
Mou, Z., Zhang, H., Liang, S., 2020. Reliability optimization model of stop-skipping bus operation with capacity constraints. J. Adv Transp.
Muñoz, J.C., Soza-Parra, J., Raveau, S., 2020. A comprehensive perspective of unreliable public transport services' costs. Transp. A Transp. Sci. 16, 734–748.
Nair, G.S., Bhat, C.R., 2021. Sharing the road with autonomous vehicles: Perceived safety and regulatory preferences. Transp. Res. Part C Emerg. Technol. 122, 102885 https://doi.org/10.1016/j.trc.2020.102885.
Nemoto, E.H., Jaroudi, I., Fournier, G., 2020. Introducing Automated Shuttles in the Public Transport of European Cities: The Case of the AVENUE Project. Conf. Sustainable Urban Mobility. Springer 272–285.
OECD/ITF, 2014. Valuing convenience in public transport. ITF Round Tables, No. 156. OECD Publishing, F., n.d. France. France.
Osuna, E.E., Newell, G.F., 1972. Control strategies for an idealized public transportation system. Transp. Sci. 6, 52–72.
Pathak, P., Agrawal, K., Suman, H.K., Bolia, N.B., 2020. Frequency optimization-based approach for reducing crowding discomfort in Delhi bus system. Procedia Comput. Sci. 170, 265–272.
Pernestål, A., Darwish, R., Susilo, Y., Nen, E.C.P., Jenelius, E., Hatzenbühler, J., Hafmar, P., 2018. SARA1 Results Report Shared Automated Vehicles-Research & Assessment in a 1st Pilot. ITRL-Integrated Transp. Res. Lab. KTH Roya l Inst. Technol, Sweden.
Qin, F., 2014. Investigating the in-vehicle crowding cost functions for public transit modes. Math. Probl. Eng. 2014.
Rietveld, P., Bruinsma, F.R., Van Vuuren, D.J., 2001. Coping with unreliability in public transport chains: a case study for Netherlands. Transp. Res. Part A Policy Pract. 35, 539–559.
Sadrani, M., Tirachini, A., Antoniou, C., 2022. Vehicle dispatching plan for minimizing passenger waiting time in a corridor with buses of different sizes: model formulation and solution approaches. Eur. J. Oper. Res. 299, 263–282. https://doi.org/10.1016/j.ejor.2021.07.054.
Sae, 2018. Taxonomy and definitions for terms related to driving automation systems for on-road motor vehicles. SAE Int, Warrendale, PA, USA.
Salonen, A.O., 2018. Passenger's subjective traffic safety, in-vehicle security and emergency management in the driverless shuttle bus in Finland. Transp. policy 61, 106–110.
Sánchez-Martínez, G.E., Koutsopoulos, H.N., Wilson, N.H.M., 2016. Real-time holding control for high-frequency transit with dynamics. Transp. Res. Part B Methodol. 83, 1–19. https://doi.org/10.1016/j.trb.2015.11.013.
Schmidt, A., Muñoz, J.C., Bucknell, C., Navarro, M., Simonetti, C., 2016. Increasing the Speed: Case Study from Santiago, Chile. Transp. Res. Rec. 2539, 65–71.
Shang, H.-Y., Huang, H.-J., Wu, W.-X., 2019. Bus timetabling considering passenger satisfaction: an empirical study in Beijing. Comput. Ind. Eng. 135, 1155–1166.
Soza-Parra, J., Raveau, S., Muñoz, J.C., Cats, O., 2019. The underlying effect of public transport reliability on users' satisfaction. Transp. Res. Part A Policy Pract. 126, 83–93.
Suman, H.K., Bolia, N.B., 2019. Mitigation of overcrowding in buses through bus planning. Public Transp. 11, 159–187.
Sun, A., Hickman, M., 2005. The real–time stop–skipping problem. J. Intell. Transp. Syst. 9, 91–109.
Sun, L., Tirachini, A., Axhausen, K.W., Erath, A., Lee, D.-H., 2014. Models of bus boarding and alighting dynamics. Transp. Res. Part A Policy Pract. 69, 447–460. https://doi.org/10.1016/j.tra.2014.09.007.
Talbi, E.-G., 2009. Metaheuristics: from design to implementation. John Wiley & Sons.
Tian, Q., Lin, Y.H., Wang, D.Z.W., 2020. Autonomous and conventional bus fleet optimization for fixed-route operations considering demand uncertainty. Transportation (Amst). 1–29.
Tirachini, A., 2014. The economics and engineering of bus stops: Spacing, design and congestion. Transp. Res. Part A Policy Pract. 59, 37–57. https://doi.org/10.1016/j.tra.2013.10.010.
Tirachini, A., Antoniou, C., 2020. The economics of automated public transport: Effects on operator cost, travel time, fare and subsidy. Econ. Transp. 21, 100151.
Tirachini, A., Hensher, D.A., Rose, J.M., 2013. Crowding in public transport systems: effects on users, operation and implications for the estimation of demand. Transp. Res. Part A: Policy Pract. 53, 36–52.
Tirachini, A., Hensher, D.A., Rose, J.M., 2014. Multimodal pricing and optimal design of urban public transport : the interplay between traffic congestion and bus crowding. Transp. Res. PART B 61, 33–54. https://doi.org/10.1016/j.trb.2014.01.003.
Tirachini, A., Hurtubia, R., Dekker, T., Daziano, R.A., 2017. Estimation of crowding discomfort in public transport: Results from Santiago de Chile. Transp. Res. Part A Policy Pract. 103, 311–326. https://doi.org/10.1016/j.tra.2017.06.008.
Tirachini, A., Sun, L., Erath, A., Chakirov, A., 2016. Valuation of sitting and standing in metro trains using revealed preferences. Transp. Policy 47, 94–104.
Tyrinopoulos, Y., Antoniou, C., 2008. Public transit user satisfaction: Variability and policy implications. Transp. Policy 15, 260–272.
Van Lierop, D., Badami, M.G., El-Geneidy, A.M., 2018. What influences satisfaction and loyalty in public transport? A review of the literature. Transp. Rev. 38, 52–72.
van Oort, N., 2016. Incorporating enhanced service reliability of public transport in cost-benefit analyses. Public Transp. 8, 143–160.
van Oort, N., 2014. Incorporating service reliability in public transport design and performance requirements: International survey results and recommendations. Res. Transp. Econ. 48, 92–100.
Wadud, Z., 2017. Fully automated vehicles: A cost of ownership analysis to inform early adoption. Transp. Res. Part A Policy Pract. 101, 163–176.
Wang, J., Sun, L., 2020. Dynamic holding control to avoid bus bunching: a multi-agent deep reinforcement learning framework. Transp. Res. Part C Emerg. Technol. 116, 102661.
Wang, Y., Tang, T., Ning, B., van den Boom, T.J.J., De Schutter, B., 2015. Passenger-demands-oriented train scheduling for an urban rail transit network. Transp. Res. Part C Emerg. Technol. 60, 1–23. https://doi.org/10.1016/j.trc.2015.07.012.
Wardman, M., 2004. Public transport values of time. Transp. Policy 11, 363–377. https://doi.org/10.1016/j.tranpol.2004.05.001.
Wardman, M., Whelan, G., 2011. Twenty years of rail crowding valuation studies: evidence and lessons from British experience. Transp. Rev. 31, 379–398.
Whelan, G., Crockett, J., 2009. An investigation of the willingness to pay to reduce rail overcrowding, in: Proceedings of the First International Conference on Choice Modelling, Harrogate, England. Citeseer.
Wu, W., Liu, R., Jin, W., 2017. Modelling bus bunching and holding control with vehicle overtaking and distributed passenger boarding behaviour. Transp. Res. Part B Methodol. 104, 175–197.
Yap, M., Cats, O., 2021. Taking the path less travelled: Valuation of denied boarding in crowded public transport systems. Transp. Res. Part A Policy Pract. 147, 1–13.
Yap, M., Cats, O., van Arem, B., 2020. Crowding valuation in urban tram and bus transportation based on smart card data. Transp. A Transp. Sci. 16, 23–42.

Zhang, J., Yang, H., Lindsey, R., Li, X., 2020a. Modeling and managing congested transit service with heterogeneous users under monopoly. Transp. Res. Part B Methodol. 132, 249–266.
Zhang, L., Huang, J., Liu, Z., Vu, H.L., 2020b. An agent-based model for real-time bus stop-skipping and holding schemes. Transp. A Transp. Sci. 1–33.
Zhang, W., Jenelius, E., Badia, H., 2019. Efficiency of semi-autonomous and fully autonomous bus services in trunk-and-branches networks. J. Adv. Transp.
Zhao, J., Bukkapatnam, S., Dessouky, M.M., 2003. Distributed architecture for real-time coordination of bus holding in transit networks. IEEE Trans. Intell. Transp. Syst. 4, 43–51. https://doi.org/10.1109/TITS.2003.809769.